RETROFITTING OF SEISMICALLY DEFICIENT REINFORCED CONCRETE (RC) CIRCULAR BRIDGE PIER USING CFRP JACKETING

By

HUSNAIN MOHY UD DIN

NUST-MS-SE 00000203989

MS STRUCTURAL ENGINEERING

THESIS SUPERVISOR

LT COL. DR. MUHAMMAD RIZWAN

Military College of Engineering, Risalpur

National University of Sciences and Technology, Islamabad

2021

It is certified that the

Master's Thesis Work titled

RETROFITTING OF SEISMICALLY DEFICIENT REINFORCED CONCRETE (RC) CIRCULAR BRIDGE PIER USING CFRP JACKETING

Submitted by

HUSNAIN MOHY UD DIN

MS SE 00000203989

has been accepted towards the requirements for

Master of Science

in

Structural Engineering

_____

Dr Muhammad Rizwan

Associate Professor

Military College of Engineering, Risalpur

National University of Sciences and Technology, Islamabad, Pakistan

Dedicated to

My Late Father, Mother and Siblings

ACKNOWLEDGEMENTS

All praises for Allah who blessed me with knowledge, spirit and dedication to perceive, execute and carry out this research work; and millions of Darud-o-Salam to His Prophet Hazrat Muhammad (PBUH). I am deeply grateful to my parents for their financial, moral support and suggestions towards my progress in life. Without their prayers it would have not been possible for me to succeed.

I would like to pay debt of gratitude to my advisor Dr. Muhammad Rizwan whose countless inspiration and guidance made it possible to complete my research work. I am also extremely grateful to committee members, Dr. Syed Hassan Farooq and Dr. Muhammad Shahid Siddique for their immense support and assistance in completing my thesis.

I also want to sincerely thank my research fellows Waleed Khalid, Muhammad Ahmed and Lab Engr. Huzaifa Umer Farooq, Lab Asst. Fayyaz and Zeeshan, all my colleagues and class fellows for enabling me to successfully accomplish my targeted goals during the course of my research work.

Table of Contents

LIST OF FIGURES

LIST OF TABLES

ABSTRACT

The bridge piers of old bridges are often found deficient either due to increased load class of traffic or damages caused by various reasons. In some cases the seismic requirements are found lacking due to poor detailing or ignorance of seismic effect at time of design and construction of bridge piers. Seismic performance is affected by material properties, quantity of longitudinal and transverse reinforcement, external confinement, axial load and shear span-depth ratio. These parameters are considerably different in the pre-1970 provision of code as compared to the current seismic requirements. Various retrofitting techniques have been developed which can enhance the strength and ductility of RC bridge piers.

This research is intended to examine the efficacy of one such strengthening technique, involving the use of carbon fiber reinforced polymer (CFRP) jackets in plastic hinge region, in enhancing the displacement capacity and strength of bridge piers. In addition, nonlinear reverse cyclic testing and analysis are carried out in order to determine the lateral load carrying capacity, flexural ductility, and hysteretic behavior of such retrofitted piers.

Chapter 1

Introduction

1.1 Background

In comparison to buildings, bridges are less redundant and thus they have limited potential of avoiding total collapse through the distribution of damage to a large number of plastic zones within the structure. Indeed, collapse of a single beam/span and, even more, of a column will most probably result in failure of the complete structure. In addition, most bridges are valuable during the immediate post-earthquake emergency, since they are required to ensure transport of heavy machinery, first-aid supplies and eventual victims between earthquake-struck and surrounding areas. Being parts of complex communication lifelines, bridges need to maintain a high level of occupancy, even in the event of a strong earthquake. This is contrary to normal buildings for which significant, but repairable, damage is accepted. Severe earthquake-induced damage on bridges results in economic losses in the form of repair, or replacement, costs and disruption of traffic. The above explain why particular attention and special studies are dedicated to bridges, even though in most cases they can be considered as simple plane-frame structures. Field and experimental observations allowed to identify the main seismic deficiencies of existing bridges. They concern the abutments, deck, columns, cap beams and foundation elements. Considering columns in particular, the most common problems are the limited shear strength, presence of lapped splices in the critical zones, limited ductility capacity and premature termination of longitudinal reinforcement. It is argued that older bridge piers were designed with focus on strength rather than deformation and without provisions to ensure stability of the response in the post-elastic range (Pinto & Monti, 2000). These observations support the need for retrofit and also provide guidance on the targets to be sought. Rectangular, octagonal, circular or wall-type solid cross-sections are often used for bridge piers. In the case of tall piers, it is desirable to reduce the mass of the pier and consequently the seismic loads it has to resist. In the USA the trend is to use solid sections and to reduce the cross-sectional dimensions with height. In contrast, piers with rectangular hollow cross-section are commonly used in Japan and Europe for highway bridges that cross deep valleys (Hooks, et al., 1997). Despite the large population of existing bridge

piers with solid cross-section, their seismic performance and appropriate retrofit techniques have not been extensively studied until recently. This provided the motivation to focus the research presented herein to the assessment and retrofit of bridge piers with solid circular bridge piers.

1.2 Problem Statement

The aim of this study is to evaluate, experimentally and numerically, the seismic performance of reinforced concrete bridge piers with jacketing of CFRP as a transverse reinforcement. For that purpose a column specimen is selected which is already tested to its ultimate capacity. The specimen is repaired with market available concrete and steel strengthening epoxies. Then jackets of fiber reinforced polymer are applied in its plastic hinge region which is the most critical one. The column specimen is tested under quasi static cyclic test to check its capacity performance and seismic behavior of CFRP jackets and compare it with the already tested specimen.

1.3 Aims and Objectives

Objectives of this study will mainly focus on achieving following goals.

a. To work out a suitable repair procedure and develop a retrofit strategy for restoration of a damaged RC bridge pier.

b. To experimentally investigate the effect of retrofitting on dynamic properties of ¼ scaled-down cantilever specimen when subjected to cyclic lateral loads under constant axial loading.

c. To compare the strength, ductility and energy dissipation capacity of retrofitted specimen with original specimen.

1.4 Scope

RC piers of bridges located in earthquake-prone regions are subjected to large force demands during strong seismic shaking, which in turn can lead to large deformations. The capacity and deformability of these piers depends heavily on the reinforcement detailing, and in particular on the confinement. Previous research has investigated the use of internal steel stirrups and spirals to enhance the seismic behavior of cantilever columns and pier-

like specimens. The other way to enhance the seismic capacity of piers by applying the external jackets covering the whole length or in the critical deformation section. The scope of this research covers the study of different retrofitting techniques mainly focus on the carbon fiber reinforced polymer jackets as a transverse reinforcement in the plastic hinge region. This study focuses on the key performance parameters of sold circular bridge piers under cycling loadings and their behavior after repairing and retrofitting. This article contributes towards developing new and more effective confinement solutions for RC piers of bridges built in seismic-prone developing countries.

1.5 Significance of the Study

Following the 2005 Kashmir Earthquake, Ministry of Housing and Works issued 'Building Code of Pakistan; Seismic Provisions' in 2007 (Ministry of Housing & Works, 2007). In addition, Pakistan Meteorological Department (PMD) issued 'Seismic Hazard Analysis and Zonation for Pakistan, Azad Jammu and Kashmir' (PMD & Norsar, 2007). The revised seismic zoning map divided Pakistan into five seismic zones named as Zone 1, 2A, 2B, 3 and 4, in order of increasing quantifiable Peak Ground Acceleration (PGA) values. Since then, designers would certainly have utilized these PGA values for seismic design of structures.

The multi-billion CPEC is a collection of infrastructure projects that are under construction throughout Pakistan. Gwadar, which is located close to Makran Trench, last saw a huge earthquake of 8.1 magnitude in 1945, killed around 4000 people. The trench is the meeting point of two tectonic plates. Along with seismic activities, CPEC road infrastructure will witness increase load class of traffic in near future. Under construction bridges need to be built considering seismic measures. Pakistan also needs to revise its bridge design code of 1967, which is lacking current seismic requirements. This experimental study will help to develop a structurally recommendable and financially viable means of construction and retrofitting techniques in case of damages.

Pakistan needs to revise its bridge design code of 1967 such that the PGA values given in seismic hazard map of 2007 (PMD & Norsar, 2007) are utilized, displacement-based

design procedure given in 2nd edition of AASHTO Guide Specifications for LRFD Seismic Bridge Design (AASHTO, 2011) is endorsed for design of bridges, and findings of report titled 'Seismic Design of Bridge Columns based on Drift' (ACI Committee 341, 2016) are incorporated. This research is intended to advance knowledge on devising a reasonable retrofit technique. In addition, it is aimed at outlining a procedure for repair and retrofit of bridge piers. Particularly, this experimental investigation is intended to develop a structurally recommendable and financially viable means of retrofitting the existing bridge piers.

1.6 Thesis Organization

Second chapter deals with the literature review of seismic history of bridges, seismic hazards and its implications and experimental testing of bridge piers. Third chapter deals with the instrumentation and calibration of equipment used for the quasi cyclic testing. Chapter 4 of this research is focused on methodology and materials used in the preparation for the modeling of specimen and methodology used to test the specimen. Last part describes the experimental results obtained from cyclic test on specimen column.

Chapter 2

Literature Review

2.1 Introduction

This chapter provides a brief overview of the literature relevant to the study conducted for this dissertation. It covers topics such as experimental testing programmes, numerical modelling of inelastic nonlinear structures, and the history of seismic design of bridges following a significant earthquake. The literature study on testing of structures is offered, with a focus on bridges specifically. The primary testing method employed in this work is quasi-static testing, which is also reviewed.

The inelastic nonlinear time history analysis is discussed in this section. The foundation of this study is a variety of hysteretic models, which are briefly reviewed. Different hysteresis models that have been previously proposed contain hysteretic modelling factors incorporating stiffness decay, strength degradation, and pinching. With particular reference to bridges, hysteresis curves and response modified factors are also discussed.

2.2 History of Seismic Design of Highway Bridges

In the majority of the developed World, extensive studies on the seismic designs of bridges started a few decades ago. According to historical records, Japan was a pioneer in the creation of seismic design guidelines for highway bridges. The first set of seismic rules, which recommended including lateral loads equivalent to 20 % of the total self-weight for highway bridges after the devastating Great Kanto Japanese earthquake in 1923, were released in 1926. (Kawashima, 2000). The first complete seismic design guidelines were not established in Japan until 1971. (JRA, 1971). The seismic design standards were further revised in 1980, 1990, 1996, and 2003. (Ali, 2009).

In the United States (U.S.), seismic design provisions/guidelines— recommending inclusion of lateral load equal to 2% to 6% of total load depending on type of foundation— were first mentioned in 8th edition of AASHTO Standard, published in 1961 (Wang, 2004). Since then, remarkable evolution in theory and practice has taken place and as of most

recently, 2nd edition of AASHTO Guide Specifications for LRFD Seismic Bridge Design (AASHTO, 2011), recommends displacement-based design procedure instead of traditional force-based R-Factor method for seismic design of bridges. Another recent development in this regard is the report published by ACI Committee 341 in 2016, titled 'Seismic Design of Bridge Columns based on Drift' (ACI Committee 341, 2016). As a consequence, bridges designed and constructed in the past may not come up to the design requirements of modern/revised codes specifications that have been radically revised (Wang, 2004; Yalcin, 1998).

In 1960s, the Government of Pakistan hired Howard, Needles, Tammen & Bergendoff (HNTB) Corporation, an American infrastructure design firm, to prepare code of practice for highway bridges in Pakistan. As a result, first bridge design code was published in 1967 (Highway Department, 1967). However, the seismic design guidelines that were included in the code were taken from 11th edition of AASHTO Standard, published in 1961. One of the most crucial requirements was that bridges be designed to withstand a lateral load between 2 and 6 percent of the total dead load.

AASHTO Standard is primarily used in Pakistan for bridge design. But in terms of seismic hazard, there have been abnormalities. The Pakistan Building Code of Earthquake Provisions (BCP, 2007), which was published in 2007, was the first to quantify the seismic danger as Peak Ground Acceleration (PGA). The 475-year return period served as the foundation for the 2007 Seismic Hazard Map. In the past, earthquake intensity maps based on the Modified Mercalli Intensity (MMI) scale were published, but they lacked particular PGA values. As a result, random PGA values were employed in the design of old bridges.

2.3 Seismic Hazard in Pakistan and its Implications

The Geological Survey of Pakistan (GSP) created the Map of Seismic Hazard that was in use until 2007. It was established on instrumental Macro-Earthquake data from the Geophysical Center Quetta from 1905 to 1979, and the Seismic Zoning was based on the Modified Mercalli Intensity (MMI) Scale (BCP, 1986). Since it is derived on visual inspections of damage at a particular region and is linked to the nature of the structure at that site, the MMI scale is unable to provide a quantitative evaluation of the peak ground

amplitudes and may only generate rough approximations of the ground shaking intensities. However, a complex design and construction scenario is created when the AASHTO Standard Specification is used in isolation from local conditions like material properties, workmanship, and construction practices. Additionally, if the region's collection of earthquake records grows, it may be necessary to update the seismic hazard map, which would necessitate reassessing any bridges that have previously been built. After the M7.9 Great Kanto Earthquake in 1923, the seismic design of bridges in Japan received serious consideration. From 1923 to 1995, only 15 bridges collapsed as a result of earthquakes, indicating a trend toward fewer bridge failures as well as the maturation of design experience accumulated over time. However, the 1995 Hanshin/Awaji Earthquake in Kobe alone resulted in the destruction of 25 bridges (Kawashima and Unjoh, 1996), leading to a revision of the Japanese bridge seismic code. After the disastrous earthquake that struck Pakistan on October 8, 2005, a laborious process of creating a seismic code for structures was initiated, and BCP was eventually published as a result (BCP, 2007). This code's Chapter 2 discusses seismic hazards, and according to that section, the Design Based Ground Motion has a 10% chance of being exceeded within 50 years. From the BCP Seismic Hazard Map (BCP, 2007), it is clear that the vast majority of Pakistan is located in Seismic Zone 2A or higher, which is associated with Peak Ground Accelerations (PGAs) of 0.08–0.16 g..

Prior seismic zoning in Pakistan relied, as mentioned, on an MMI scale developed in 1931. This MMI-derived seismic zoning map classifies Pakistan into four distinct regions based on their relative susceptibility to earthquakes: Zone 0 (the least prone), Zone 1 (moderate), Zone 2, and Zone 3. Unfortunately, the level of shaking that can be detected by this map is not measurable. Zone 2 encompasses most of the northern region of Pakistan and is classified as a moderate damage area (MMI VII). Balakot, Muzaffarabad, etc. in northern Pakistan is located in the vicinity of greatest possible seismic events, i.e., Zone 4 with the a PGA 0.32g, according to the recently published Seismic Risk Map in BCP (BCP, 2007) with five Seismic Zones, numbered Zone 1, Zone 2A, Zone 2B, Zone 3, and Zone 4, in sequence of increasing ground acceleration. The remaining portion of the north is classified as Zone 3, which has a PGA between 0.24g and 0.32g. All newly constructed buildings must be built to withstand higher earthquake loading in accordance with the new

Earthquake Risk Map, and existing buildings may require retrofitting to meet these new standards. The bridges must also be structured for a lateral loads equivalent to 2% to 6% of the load capacity of the structure, as specified by the 1967 Code of Procedure for Highway Bridges (CPHB, 1967). Multiple foundation types resting on a wide variety of soil profiles produce settlement patterns in the 2–6 percent range. Since the CPHB was written before the seismic zoning map was made available, it can be followed without regard to that data. The 1967 Building Code must be updated to reflect the latest Seismic Hazard Map and its associated specifications.

The AASHTO Standard Specification, which is based on the United States Geological Survey's Seismic Hazard Map, has been widely used in the planning and construction of bridges across Pakistan. This means that for bridges built before 1979, lateral forces were calculated using values between 2% and 6% of the bridge's total weight, or else arbitrary PGA values were used. The Seismic Hazard Map, which is rooted on the MMI scale but lacks quantifiable PGA values, was used for bridge designs from 1979 through 2007. Therefore, the designers used completely arbitrary PGA values. The Earthquake Risk Map released in (BCP, 2007) with pertaining PGA values depends on a 10% possibility of exceedence in five decades is necessary for the assessment and rehabilitation of existing bridges. Remember that the 1980s AASHTO Standard allowed for the use of overly simplistic elastic design methods like the Equivalent Static Force Method and the Response Spectrum Method. Even so, the current AASHTO-LRFD approach incorporates a number of different types of analysis, such as the linear/nonlinear response history analysis, which can be applied to both elastic and inelastic materials. The regularity or unevenness of a bridge plays a role in how the analysis method is selected in conjunction with the bridge's importance and its location within a given seismic zone.

It is crucial to assess the current bridges in order to prepare for potential earthquakes. The 1967 Bridge Code needs to be significantly revised, and practice on an indigenous bridge code requirements should begin immediately. Large portions of Pakistan, including those near major cities like Quetta, Karachi, Peshawar, Gwadar, Abbottabad, Gujrat, and Islamabad, are located in seismically active zones, as shown by the BCP Seismic Hazard Map (BCP, 2007). Rapid progress in infrastructure development means that the updated

Earthquake Risk Map must be used for all future bridge construction and all necessary retrofits.

2.4 Seismic Testing Methods

The purpose of the research should be taken into consideration when selecting an appropriate testing strategy from among several possibilities. Experiments can be either static, quasi-static, pseudo-dynamic, or dynamic. All tests may be performed in a single lab, but the required size of the necessary equipment varies widely. In most cases, you'll only have a few options when deciding on a specimen size and/or test type. Once a lab has made a financing, such as purchasing expensive equipment, a researcher may find themselves working within a stricter financial constraint. Time is typically another limitation on testing, dictating such factors as the maximum size of a test specimen and the maximum number of samples that can be tested. There is only a weak correlation between specimen size and testing time; reduction in the size of the specimen too much could result in unreasonably long delays when compared to using a larger specimen. The difficulty of accurately fabricating such tiny parts and the general scarcity of such components may be to blame. The duration of a test takes into account not only the time spent actually performing the exam, but also the time spent on everything from planning the test to analyzing the data collected from the test. Although the duration of the actual testing itself may be quite short—only seconds in the case of dynamic testing or days in the case of static testing—it is usually much longer than the actual duration of the experimental investigation.

There are two type static tests; one is the monotonic and other one is cyclic tests. Both shaking tables tests and tests with exciters such simple linear vibrators and eccentric large mass vibrators fall under the category of dynamic tests. Pseudo-dynamic testing is a type of testing that takes place in between the two extremes of dynamic testing and static testing, and it involves complicated computations to account for inertial forces from dynamic testing.

There are other, more complex types of testing, such hybrid distributed testing, which involves testing a portion of a structural components both digitally and physically in the lab, with the testing locations being spread across several regions. Every testing technique,

thus, has advantages and disadvantages of its own; nonetheless, the selection of a technique depends on the trial objectives.

Quasi-static testing typically costs less money, requires less specialized equipment, and doesn't need a lot of hydraulic fluid to produce immediate forces and displacements. There is sufficient time to watch and notice changes during these examinations. The ease with which huge specimen can be tested is another significant benefit. The rate impacts are not tested, which is a limitation (Sullivan, and Pavese, 2004).

Not the price of the specimen itself, but rather the cost of running the shaking table, is what makes dynamic testing so prohibitively expensive. The rate impacts are considered, and the input to the shake table, often an earthquake time history, is representative of the actual input a structure would encounter during testing (Sullivan, Pavese, and Pinho, 2004); (Harris and Sabnis, 1999). There are various issues related with shaking table testing. There are many challenges associated with testing huge structures, such as the difficulty of control, the difficulty of observing the sequence of events leading up to structural failure, and the short time frame. There aren't many shake tables that can handle heavy loads.

2.5 Experimental Testing of Bridges

In comparison to buildings, bridges typically have a large supported mass. For example, a pier supporting a two-lane, pre-stressed girder bridge spanning 25 to 28 metres (82 to 92 feet) would be subject to a load of 300 to 400 metric tonnes (661-882 kips). Even if scale models were to be examined in a laboratory, the massive size of the mass and geometrical dimensions would necessitate extensive testing facilities.

Quasi-static testing is one common method used to evaluate bridge column strength. In addition to the aforementioned benefits, quasi-static testing also makes it simpler to test a component.

Sheikh evaluated 56 bar specimens with monotonic loading, using the findings of the tests to offer a numerical method for forecasting the behaviour of plastic hinges (Sheikh, 1978). The concrete strength of the columns measured by Sheikh (Sheikh, 1978) ranged from 3,540 psi to 5,932 psi.

Zahn and others (1989) conducted set of tests on concrete columns to examine its strength and ductility, the strength of the material ranged from 3,400 psi to 5,200 psi.

Cheok and Stone (1990) investigated the effect of varying the axial load, aspect ratio, and material type on the behavior of six 1:6 scale circular concrete bridge piers applied to quasi-static cyclic loading. The columns' concrete strength was near to 4,000 psi.

Some studies have done full-scale dynamic analysis of bridges but generally confined to ambient vibration analyzing tests and/or forced vibration testing utilizing external exciters for the aim of finding the natural time periods, modal geometries and modal damp proportions (Salawu and Williams, 1993).

Twenty-seven RC columns with concrete strengths ranging from 5,000 psi (34.9 MPa) to 5,200 psi (35.9 MPa) were subjected to monotonic axial compression tests conducted by Sheikh and Toklucu (Sheikh and Toklucu, 1993). The type and amount of lateral steel, lateral steel spacing, and specimen size were among the variables studied to determine their impact.

The research conducted by Priestley and Benzoni (1996) on two full scale reinforced concrete solid circular piers with limited longitudinal reinforcement and after tests they concluded the concrete strength of 4,350 psi.

There were 31 different types of concrete column specimens tested, each with its own unique dimensions and reinforcements to see which would be best for use in bridge columns (Hoshikuma et. al., 1997). This study used a concrete strength spectrum from 2,680 psi to 3,500 psi. Contrarily, the 2,680 psi (18.5 MPa) concrete columns had a diameter of 7.9 in (200 mm), a length of 23.6 in (600 mm), and confining steel was given; however, there was no longitudinal reinforcement.

Twelve specimens of scale 1:4 circular concrete bridge piers were put through cyclic loading tests. The strengths of the concrete ranged between 5,200 psi (36.0 MPa) and 5,800 psi (40.0 MPa) concluded by (El-Bahy A. et. Al., 1999). These tests was done for examining the cumulative destruction to RC bridge columns built in accordance with AASHTO standards. The impact of varying amplitude loads on the columns response has also been investigated by the researchers. (Kunnath, Stone, Taylor, and El-Bahy, 1999).

Approximately 50 concrete bridge piers have been examined in Japan by Kawashima and others using quasi-static techniques. Testing was done to determine, among other things, how interlocking connections affected strength and ductility, how loading hysteresis affected ductility, and how long plastic hinges should be. These columns' concrete strength ranged from 2,900 psi and ends till 5,330 psi.

Bayrak and Sheikh investigated the plastic hinge location analysis in reinforced concrete piers (Bayrak and Sheikh, 2001).

Mo and Nien (2002) examined the seismic performance of hollow bridge columns. They evaluated six bridge columns made of concrete with strengths ranging from 7,200 psi till 10,000 psi under quasi-static loading.

Four models and two prototypes were put through a second round of quasi-static testing on bridge columns by (Mo and Yang, 2002). Their research resulted in columns' concrete strength ranged between 4,200 psi till 4,900 psi.

(Bae and Bayrak, 2008) conducted full-scale testing of 5 concrete bridge piers to examine their seismic performance. Cyclic testing was carried out by Bae and Bayrak with a constant axial load. The columns' concrete strengths ranged from 4,350 psi to 6,400 psi.

Chapter 3

Instrumentation and Calibration

3.1 General

The chapter describes the material properties and geometry of trial steel column, fabricated to develop familiarization with the relevant laboratory equipment. A study related to specifications of instruments used in the experimental work is also presented.

3.2 Study of Lab Instruments

The study of instruments involved working out procedures of use, fixing threshold parameters in respect of capacities of instruments and calibration. This activity was carried out by testing a steel column.

The Structural Engineering Laboratory at Military College of Engineering, Risalpur has all the necessary instruments required for Quasi-Static Cyclic Testing. In addition to calibrating the equipment, the primary objectives of this exercise were to develop understanding and learn the instrumentation process and conclude experimental results by means of testing a trial steel column.

3.2.1 Quasi-Static Cyclic Test

To test the trial steel column, special type structural frame assembly was used, as presented in Figure 3.1, comprises of space frame having adjustable girders that may be used to change the position of actuator, hydraulic jack and test specimen within the frame. The actuator has the capacity of 25 metric ton while hydraulic jack has the capacity of 50 ton. The specifications of actuator and hydraulic jack are presented in Table 3.1 and Table 3.2, respectively.

A trail steel column was fabricated in order to investigate how the quasi-static cyclic testing system functions. The cross section of trial column is shown in Figure 3.4. Table 3.3 describes the geometry of trial steel column and its material properties.

3.2.2 Testing Methodology

A detailed testing procedure was developed in order to test the trail steel column. A vertical hydraulic jack was used to simulate the effect of dead mass on top of the column, and two horizontal actuators positioned on one of the faces of trial steel column top in the direction of cyclic loading were used to simulate lateral cyclic loading.

3.2.3 Fabrication of Trial Column

With the intention of acquiring familiarization with the testing process and equipment, a scaled trial steel column, shown in Figure 3.3, was fabricated. A steel plate was welded on the column top in order that load from the vertical hydraulic jack can be applied. Similarly, steel plates were also welded on sides of column top in order that lateral cyclic loads may be applied from the horizontal actuator.

3.2.4 Equipment Setup

Quasi-static cyclic test was carried out on trial steel column by using the setup shown in Figure 3.3. An actuator of 15 ton capacity was fixed on the horizontal girder of structural frame at an elevation such that the steel plates welded on the sides of column top can be adequately bolted to the actuator.

A small reaction frame was also fabricated in order that a displacement transducer may be fixed to it to measure the displacement in the direction of application of lateral load. The magnitude and intensity of lateral loads was documented by means of automatically attached load cells of actuators. Due to some technical issues, simulation of dead mass by means of vertical hydraulic jack was omitted at this stage of trial testing.

3.2.5 Calibration of Instruments

Prior to testing the trial steel column, load cells of actuators and displacement transducers were calibrated. The load cells were calibrated by measuring the known weight of a human.

3.2.6 Test Protocol

Column testing was performed using cyclic loading. 150 seconds (or 0.0067 Hz) was the specified time interval. Lateral load was provided by a speed-control actuator with a 15-ton capacity, which was attached to an RC reaction wall. A 25-ton load cell was installed horizontally between the actuator and the column top to measure the horizontal thrust applied to the column head. A Linear Displacement Sensor was used to measure the drift or horizontal displacement (LDS).

Lateral load will be applied in north and south direction. A pull acting in the south is referred to as a negative force, whereas a push acting in the north on the column is described as a positive force. Similarly, positive displacement describes column movement in the north and negative displacement describes movement in the south.

Quasi-static cyclic load tests are so slow that the contribution of mass in producing inertial effects is inconsiderable. The velocity of mass is also slow as a result of which damping also becomes insignificant. Consequently, the equation of motion becomes:

$$F(t) = k_i u \tag{3.1}$$

Where:

$F(t)$ is the force in lateral direction.

k_i is the inelastic stiffness of trial steel column.

u is the displacement in the lateral direction of the column measured horizontally in the plane of lateral force application.

From the Eq. (3.1) stiffness can be determined at any position by inputting the values of reaction force and corresponding displacement.

3.2.7 Testing of Trial Column

The trail column was subjected to multiple positive and negative displacements, and the corresponding reaction forces were recorded. The positive displacement refers to push of actuator, whereas the negative displacement refers to pull of actuator. Similarly, the positive force indicates push of actuator while the negative force indicates pull of actuator. Table 3.4 presents the magnitude of displacements given to the column and the corresponding forces. Figure 3.5 shows the load versus displacement graph for positive load and positive displacement of trial column.

Figure 3.6 shows the load versus displacement graph for negative load and negative displacement of trial column.

3.3 Conclusions

The study of laboratory equipment by testing and analyzing a trial steel column provided invaluable experience. All the relevant instruments responded in a rational manner during calibration. The linear relationship between reaction and displacement for positive as well as negative parts of the cycles during testing of trial column is a sound piece of evidence

that the relevant instruments are in a reasonably workable condition to go for testing of retrofitted RC bridge piers.

Figure 3.1: Structural frame used for trial steel column and actuator

Figure 3.2: Geometry of trial steel column

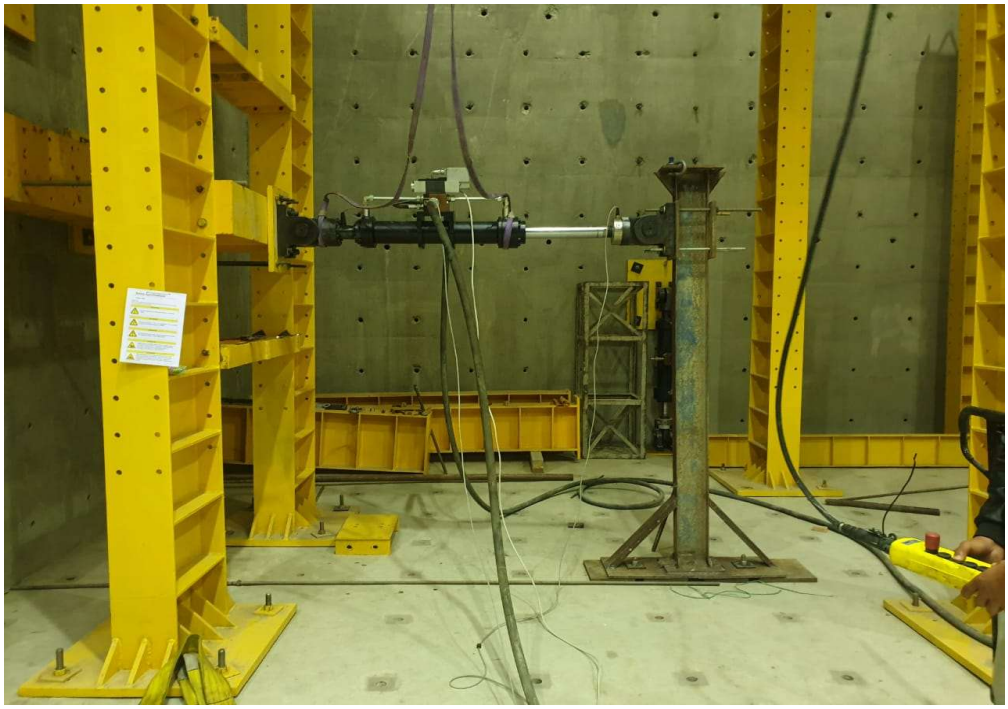

Figure 3.3: Experimental setup for quasi-static cyclic loading test on trial steel column

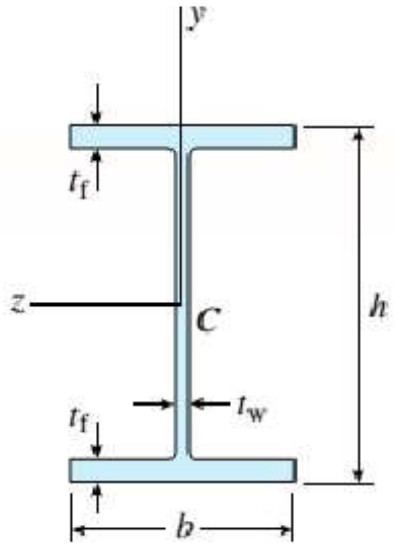

Figure 3.4: Cross section of trial column

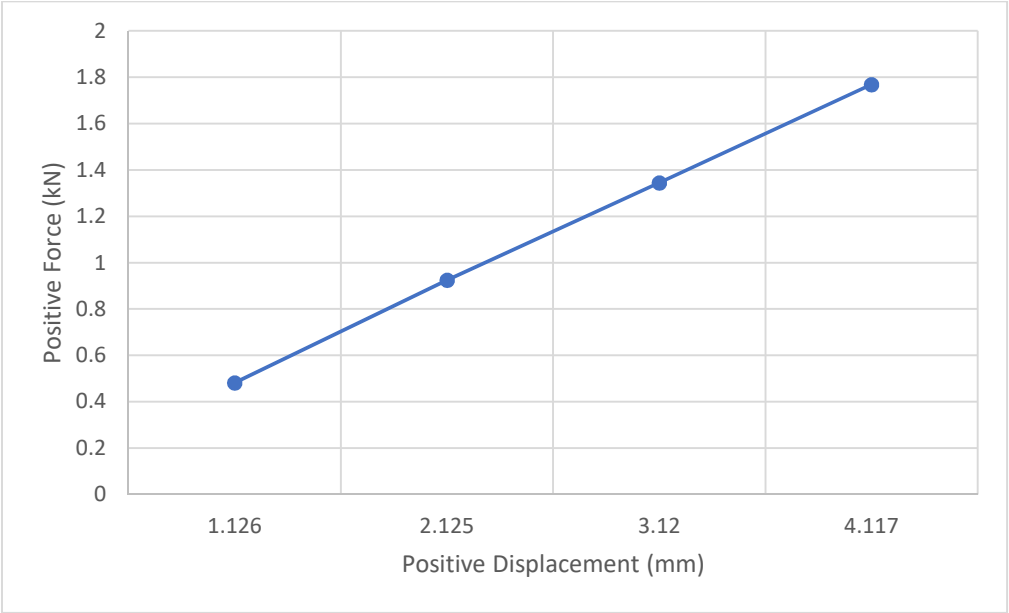

Figure 3.5: Load-displacement graph for trial column (Push of actuator)

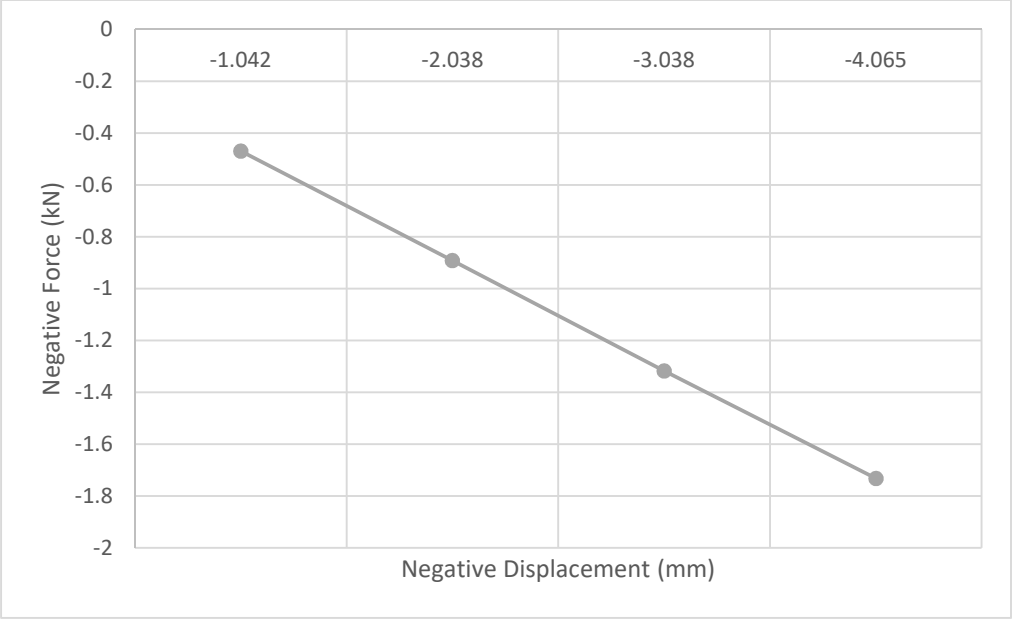

Figure 3.5: Load-displacement graph for trial column (Pull of actuator)

Table 3.1: Specifications of actuator

Actuator 25 ton	
Capacity	250 kN
Stroke	500 mm
Type	Parkor
Maximum Speed	1 m/sec
Total length	1.53 m

Table 3.2: Specifications of hydraulic jack

Hydraulic Jack 50 ton	
Capacity	500 kN
Stroke	300 mm
Type	Parkor
Maximum Speed	Manual processing
Total length	0.5 m

Table 3.3: Geometric and material properties of trial column

Property	Magnitude
Column height (in.)	74
Type of steel (ASTM designation)	A992
Tensile yield strength,f_y (ksi)	50
Tensile ultimate strength, f_u (ksi)	65
Depth of section, h (in.)	6.75
Flange width, b_f (in.)	3.375
Flange thickness, t_f (in.)	0.25
Web thickness, t_w (in.)	0.375
Moment of inertia about x-axis, I_{xx} (in.^{4})	25.46
Moment of inertia about y-axis, I_{yy} (in.^{4})	1.63
Elastic section modulus about x-axis, S_{xx} (in.^{3})	7.54
Elastic section modulus about y-axis, S_{yy} (in.^{3})	0.97
Plastic section modulus about x-axis, Z_{xx} (in.^{3})	9.15
Plastic section modulus about y-axis, Z_{yy} (in.^{3})	1.64
Torsional constant, J (in.^{4})	0.15
Warping constant, C_w (inch.^{6})	16.92
Radius of gyration about x-axis, r_{xx} (in.)	2.5132
Radius of gyration about y-axis, r_{yy} (in.)	0.6357

Table 3.4: Values of load versus displacement for trial column

Maximum Load (kN)	Maximum Displacement (mm)	Minimum Load (kN)	Minimum Displacement (mm)	Number of Cycles
0.482	1.126	-0.469	-1.042	1
0.925	2.125	-0.891	-2.038	1
1.345	3.12	-1.317	-3.038	1
1.768	4.117	-1.732	-4.065	1

Chapter 4

Modeling and Experimental Work

4.1 General

In this chapter, modeling of specimen, material properties, repairing and retrofitting strategy and experimental testing methodology is described. A single reinforced concrete solid circular bridge column section is selected for this study. The study involves the failure mechanism of the circular column which was tested earlier and the techniques which are used to repair columns and make them strengthen. The specimen was first tested to its ultimate capacity and then it is repaired and retrofitted with the help of carbon fiber reinforced polymer jackets.

The first section of this chapter contribute towards the study of characteristics of solid circular column specimen. The study of specimen involves its cross section, geometry, mass and material properties which are used for the fabrication of model. It also describes different techniques used for repair and retrofit purpose and the one which is actually used for studied section.

The second part describes the various aspects related to experimental testing and methodology used in analyzing the model specimen. The study of lab instrument includes determining the correct procedure of use, equipment setup, calibration of instrument, test protocols and testing of specimen. Final section of this chapter deals with the final testing arrangements of cyclic static test in light with scale factors and test protocols.

4.2 Model Geometry

Three ¼ scaled-down cantilever specimens were cast and subjected to cyclic load. The specimens simulated a bridge pier between contra-flexure points and were similar to those tested by Tahir et al. (Tahir et al., 2015). The pier (D=305 mm, H=1981 mm) was cast on a solid concrete base (2133×914×508 mm) that simulated a stiff bridge foundation. The main longitudinal reinforcement consisted of 26 bars of size 7.37 mm, evenly distributed along the piers' perimeter. The longitudinal bars were anchored with a 90° bend for a length of 200 mm within the base. The clear cover to the main bars was 12.2 mm. The base was

reinforced with five 12 mm bars placed parallel to the longitudinal direction, and eleven 12 mm bars along the short direction. A concrete block (305×762×762 mm) on the top of the column simulated the pier header. The transverse reinforcement used was pre-bent metal strips and the clear spacing between the transverse reinforcement was 37.5 mm. The pre-bent strip in specimen had a cross section of 1.3×12.2 mm. All confinement was closed with 135° hooks, as required by current seismic codes. Table 4.1 demonstrates the summary of model parameters. Figure 4.1 presents the comprehensive drawings of the model pier.

Table 4.1: Summary of Testing Model Parameters

Parameter	Model
Diameter	305 mm (12 in.)
Pier height	1676 mm (66 in.)
Pier concrete strength f`c	20.7 MPa (3000 psi)
Supported mass	192.4 KN (43.25 kips)
Clear cover	12.2 mm (0.5 in)
Rebar Diameter	7.4 mm (0.291 in)
Number of rebar	26
Yield strength of longitudinal bars, fyl	365 MPa (53 ksi)
Type of confinement	Pre-bent metal strips
Confinement Cross section	1.3 x 12.2 mm
Yield strength of pre-bent strips, fyt	242 MPa (36 ksi)
Centre-to-centre spacing between strips	37.5 mm (1.5 in)
Coarse aggregate size	10 mm (0.4 in)
Normalised axial load ratio	0.13

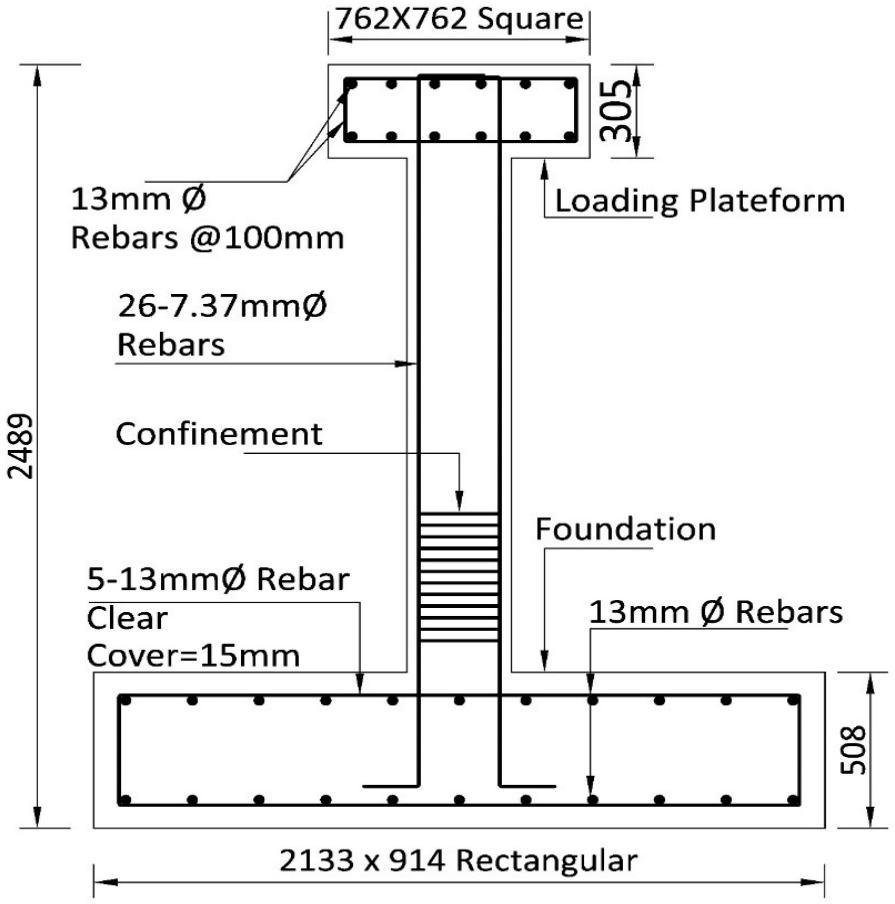

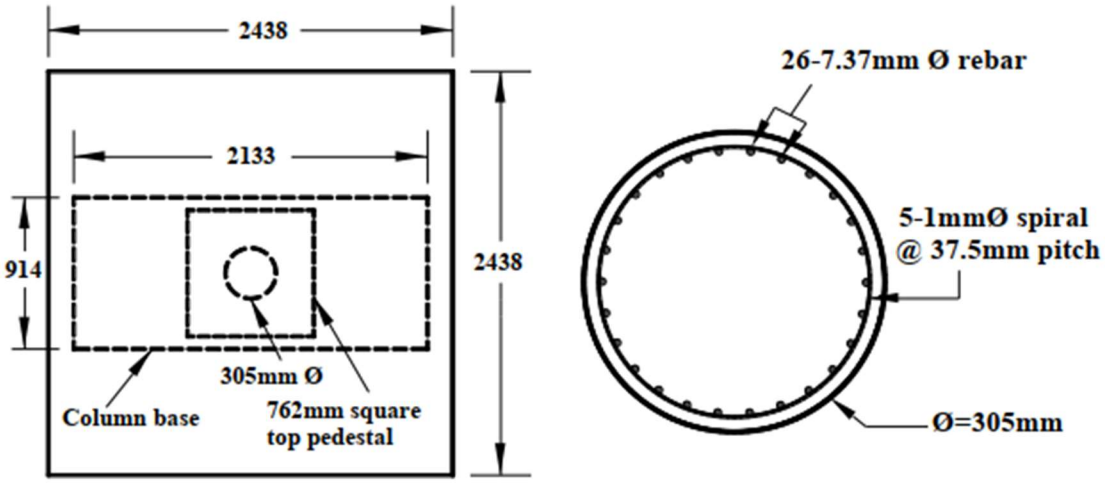

Figure 4.1: Geometric details of specimen

4.3 Model Mass

Typical prototype bridges have a mass of about 310 tons. The mass for the model is determined using a scale factor of 16 and the similitude analysis that was performed. This results in a 19.38-ton model mass requirement. Modular concrete slabs, which will be discussed in more detail in the following paragraphs are used to satisfy the model's mass need.

4.3.1 Model Material

In this section, the model materials' properties are discussed, and the properties of cement, fine aggregate, coarse aggregate, concrete mix design for dead mass of slabs used for vertical loading and properties of main and transverse reinforcement are also provided.

4.3.2 Concrete

The results by testing prototype concrete were used to create the model concrete. In order to ascertain the mechanical characteristics of concrete, a set of experimental investigations were conducted in the laboratory using concrete cubes and cylinders that were constructed and tested in accordance with ASTM provisions. For the prototype concrete, it was decided to use coarse aggregates of the same size as those applied in the field. The decision was made to reach 3000 psi (20.7 MPa) mix design based on information received from a variety of sources, including field exploration.

The existing bridges constructed in the 1970s and 1980s had compressive strength of concrete of 3,000 psi, which corresponds to cube strength, is one of the main reasons for assessing 3000 psi concrete. In this investigation, concrete was tested utilizing the cylinder-based ASTM standard (ASTMC873-04, 2004). According to Day (1999), the ratio of cube strength to cylinder strength is roughly 1.25, therefore a 3,000 psi cube would be equivalent to a 2,400 psi cylinder. It was determined to test columns with strength 25% less than 3000 psi, or roughly 2400 psi, because many bridges had weaker construction.

The crushing strength (ASTM C873-04, 2004), modulus of rupture (ASTM C78-02, 2004), and modulus of elasticity (ACI 318-02, 2001) of prototype concrete were evaluated in order to establish benchmarks for the mix design of model concrete. In order to establish similarity in the bond behavior between concrete and reinforcement, the size of coarse particles was lowered in model concrete. The model concrete that is used to prepare test

columns is described in the following sections after the prototype concrete is first discussed.

4.3.3 Fine Aggregates:

In line with the standards of ASTM, a sieve analysis of the fine aggregates used to prepare the prototype concrete was performed (ASTM C136-04, 2004). The curve from the sieve analysis is shown in Figure 4.2, and Table 4.2 lists the results.

Table 4.2: Sieve analysis data of fine aggregates ASTM C-136

ASTM Sieve #	Weight Retained (gm)	% Weight Retained	Cumulative % Retained	Cumulative % Passed
4	0.4	0.08	0.08	99.20
8	1.6	0.32	0.4	99.60
16	35.8	7.16	7.56	92.44
30	157.8	31.56	39.12	60.88
50	221.5	44.3	83.42	16.58
100	69.8	13.96	97.38	2.62
Pan	13.1	2.62	100	0

Total weight of specimen = 500 gm; Sum of cumulative % retained = 227.96

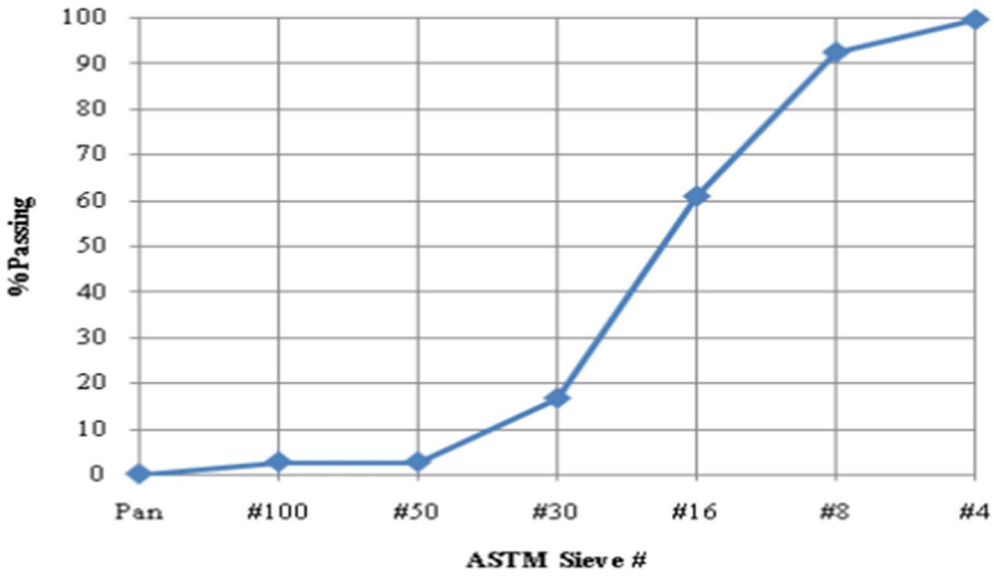

Figure 4.2: Sieve analysis curve for fine aggregates

The sand's fineness modulus was determined to be 2.3. As evaluated by ASTM (ASTM C128-04, 2004), the fine aggregates' specific gravity was 2.56 and their water absorption was 3.41%. Sand's bulk density was determined to be 151 lb/ft3 and its void ratio to be 0.018. The same fine aggregates were incorporated in the model concrete, and Table 4.3 provides a summary of these properties.

Table 4.3: Summary of properties of fine aggregates

Item	Value
Moisture content	4.5%
Void ratio	0.018
Fineness modulus	2.3
Bulk density	151 lb/ft3 (2,420 kg/m3)
Water absorption	3.41%
Specific gravity	2.56

4.3.4 Coarse Aggregates:

According to ASTM (ASTM C136-04, 2004), a sieving of the coarse aggregates for sample concrete was conducted. The results are shown in Table 4.4, and a curve is drawn in Figure 4.3.

Table 4.4: Sieve analysis of coarse aggregates ASTM C-136

ASTM Sieve #	Weight Retained (gm)	% Weight Retained	Cumulative % Passed
1.5"	0	0	100
1"	0	0	100
0.75"	0	0	100
0.5"	7	0.35	99.65
0.375"	4.9	0.245	99.40
0.25"	1,599.5	79.97	19.43
Pan	388.6	19.43	0

Total weight of specimen = 2,000 gm; fineness modulus was calculated to be 5.8.

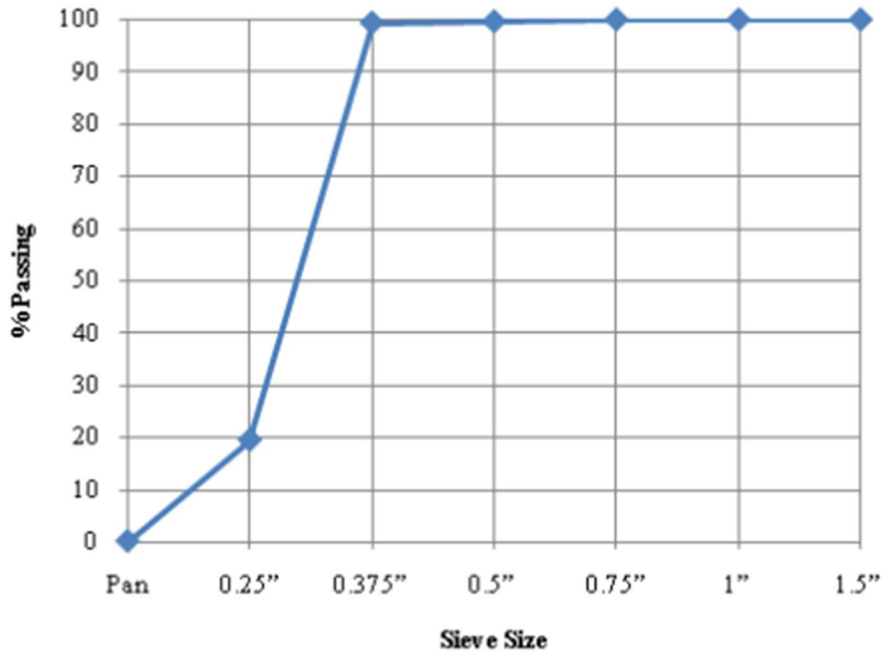

Figure 4.3: Sieve analysis curve for coarse aggregates

Water absorption was determined to be 2.53% and the specific gravity was determined to be 2.54. It was determined that the bulk density was 88.3 lb/ft3, the void ratio was 0, and the moisture content was 0.64%. Table 4.5 provides a summary of the findings.

Table 4.5: Summary of properties of coarse aggregates

Item	Value
Moisture content	0.64%
Void ratio	0.44
Bulk density	88.3 lb/ft3 (1,414 kg/m3)
Water absorption	2.53%
Specific gravity	2.54

4.3.5 Cement

In all of the model's experimental work, Type-I hydraulic cement (ASTM C150-04, 2004) was employed. Several tests were run to determine the cement's characteristics. The ASTM standard (ASTM C191-04a, 2004), from which the initial setting time was calculated to be 105 minutes and the ultimate setting time to be 216 minutes, was used to determine the cement's setting time. According to a 2004 calculation made using the light ASTM standard (ASTM C188-95(2003)), hydraulic cement has a density of 189 lb/ft3. Using the ASTM standard, the fineness of cement was reported to be 90.2%. (ASTM C117-04, 2004). The cement was found to have a 380 psi tensile strength. According to the ASTM standard (ASTM C109/C109M-02, 2004), the compressive strength of cement was discovered to be 2,590 psi. Table 4.6 provides the results synopsis.

Table 4.6: Summary of properties of hydraulic cement

Item	Value
Type	Type-I hydraulic
Initial setting time	105 minutes
Final setting time	216 minutes
Fineness	90.2%
Density	189 lb/ft3 (3,028 kg/m3)
Tensile strength	380 psi
Compressive strength	2,590 psi (17.9 MPa)

4.3.6 Mix Design for 3000 psi strength concrete:

For the model column, the ingredient weight ratios were 1:1.5:3, with a water to cement ratio of 0.62. At the time of quasi-static testing for the model column, the average strength of the cylinders evaluated in accordance with ASTM (ASTM C873 04, 2004) was 3045 psi. The experimentally determined MOR for the specimen in accordance with ASTM (ASTM C78-02, 2004) was 881 psi, while the modulus of elasticity computed from ACI (ACI 318-02, 2001) is 3459 ksi. Table 4.7 provides a summary of the findings.

Table 4.7: Concrete mix design summary

Item	Value
Proportion by weight	1:1.5:2
Water/Cement ratio	0.55
Average cylinder strength	3030 psi (20.9 MPa)
MOR	881 psi (6.07 MPa)
Modulus of elasticity	3459 ksi (23.86 MPa)

4.3.7 Fabrication of Dead Mass for Model

The column base, the column itself, the pedestal on top of the column, and the dead mass for vertical loading made up the model's four separate parts. Throughout the tests, the modular dead mass was put on each column one at a time. The plan saved time, reduced costs, and allowed for the reuse of dead material in subsequent tests.

The modular dead mass was built in the initial phase. The concrete was made using readily available aggregates, and it is strong enough to serve as a source of mass. There were mainly two kinds of RC slabs used:

a. 4ft. x 4ft. RC slabs: There were twelve of these non-structural slabs, and they were each 12 inches thick. These were intended to be non-structural slabs that could only sustain their own weight. These slabs were made using a mix of 1:2:4 cement, fine aggregates, and coarse aggregates, with a water cement ratio of roughly 0.6. The cement and coarse and fine particles utilised have the same characteristics as the prototype concrete described in earlier sections. Three rings of grade 60 reinforcement measuring 0.5 inches in diameter were employed in both directions. The combined weight of these 12 slabs was 39.91 kilos, or 71.7% of the total mass.

b. 8ft. x 8ft. RC slab: This slab, which was 12 inches thick, was structural slab. All twelve 4 foot square slabs were intended to be supported by this. The mix composition was 1:1.5:3, with a water to cement ratio of roughly 0.58. The cement and coarse and fine particles

utilized have the same characteristics as the prototype concrete described in earlier sections. To give reinforcement on top and bottom, the reinforcement was made up of 0.5 in diameter 60 grade steel bars placed 5 inches apart in both directions. This slab accounted for 24.5% of the overall bulk with a weight of 10.6 kg.

Near the four corners of the slabs, hooks were provided for lifting. The hooks were positioned in a depression so that they were flush with the slabs' top surface.

4.3.8 Model Reinforcing Steel

Steel that is commercially produced in the market was used for the model's reinforcing. Pre-bent metal strips of cross section size 1.3 x 12.2 mm were used for rebar having yield strength of 53 ksi. The model column's rebar and confinement hoops are depicted in Figure 4.4. Table 4.8 provides an overview of the steel's properties for the model.

Table 4.8: Model Reinforcing Steel Details

Group	Parameter	Model
Rebar	Type	Deformed
	Diameter	0.29 in (7.37 mm)
	Number	26
	Yield strength	53 ksi (365 MPA)
	Ultimate strength	70.4 ksi (485 MPA)
	% Elongation	20.1 %
Confinement steel	Type	Pre-bent metal strips
	Cross section	0.051x0.48 in (1.3x12.2 mm)
	Pitch	1.5 in (37.5 mm)
	Yield strength	-
	Ultimate strength	89 ksi (614 MPA)
	% Elongation	-

Figure 4.4: Pre-bent metal strips as a transverse reinforcement.

4.4 Repair and Retrofit Strategy for damaged Specimen

4.4.1 Visual Inspection of Specimen

a) Longitudinal reinforcement of column was exposed near the base of column.

b) Longitudinal reinforcement had buckled near the base of column. A few bars had also broken.

c) Concrete had deteriorated near the base of column.

d) Cracks were observed within the concrete core.

e) Spirals near the base of column were broken.

f) Flexural cracks of 1-2 mm width were observed

g) Residual displacement of approximately 70 mm was recorded in the direction of lateral loading. Similarly, residual displacement of 70 mm was recorded in the direction perpendicular to direction of lateral loading.

h) The base of the column was severely damaged and cracks were observed within the core of column. Cracks were extensive, and the concrete matrix was almost completely disintegrating.

4.4.2 Repairing of Damaged Specimen

1. The base of the specimen was rigidly attached/fixed to the structural floor of the lab using high-strength steel bolts.
2. The specimen was brought back to its equilibrium position by using actuator/hydraulic jack.
3. The disintegrated/damaged concrete was removed.
4. The transverse reinforcement of pier was adjusted.
5. The buckled longitudinal reinforcing bars of piers were straightened by hammering.
6. To achieve a sound surface, weak areas, loose material, and honeycombing were scraped off with a grinder. Compressed air was then used to clean the surface.
7. Surface primer (Sikadur 31) was used to repair the cavities and micro-cracks.
8. Epoxy mortar (Sikadur 42) was then applied for patch works.
9. Cracks within the core of pier were filled with epoxy injection (Sikadur 52).
10. Repairing process is shown in Figure 4.5, 4.6 and 4.7.

a) Bring column to zero position b) Removal of disintegrated concrete c) Adjusted pre-bent metal strips

Figure 4.5: Adjustment to zero position and surface preparation of column.

a) Application of Epoxy mortar (Sikadur 42) for patch works.

b) Cracks filling within core with epoxy injection (Sikadur 52)

c) Microcracks & cavities repaired with surface primer (Sikadur 31)

Figure 4.6: Repairing of column hinge concrete and reinforcement with sikadur epoxies.

Figure 4.7: Repaired column ready for cyclic testing.

4.5 Flexural Retrofit of Damaged Specimens

In columns, under seismic load/displacement input, confinement failure of the flexural plastic hinge area is a frequent failure mode that can be observed. In this type of failure, plastic hinge degradation is caused by concrete cover spalling and disintegration, longitudinal reinforcement buckling, or core concrete compression failure. As plastic hinge failures exhibit some displacement ductility and are limited to shorter regions in the column, they are considered less destructive and more desirable (Seible, et al., 1997).

The inelastic or non-linear deformation capacity of flexural hinge areas in existing columns can be enhanced by provision of additional confinement in form of external jacketing. The improved ductility of a section can be attributed to its capacity to cause the concrete to experience greater compressive strains before compressive collapse. The confinement provided by circular jackets can be owed to the tensile hoop strains caused by the plastic hinge's dilatation in the jacket and the pressure forces generated by the jacket curvature (Seible, et al., 1997).

CFRP wrapping can also increase the axial tensile strength and axial compressive strength of the columns. In addition, FRP wrapping can also be used to clamp the lapped splices of longitudinal reinforcing bars and slow the buckling of longitudinal steel rebars in compression (ACI Committee 440, 2017). The procedure consistent with the design guidelines presented in ACI Code 440.2R Section 11.3 has been employed for flexural hinge confinement.

4.5.1 Retrofit Objective

The first step in design of CFRP jacketing is establishment of a retrofit objective. ACI 440.2R Section 11.3 specifies that for seismic applications FRP jackets need to be built with a confining stress strong enough to produce the concrete compressive strains linked with the displacement requirements. Since retrofitting the damaged specimens to meet the displacement demands of a particular seismic zone of country is not an objective of this experimental research, an arbitrary value of desired displacement ductility is selected. Therefore, the purpose of the retrofit is to confine the CFRP jacket to the plastic-hinge region and to accomplish at least 1.5 times the displacement ductility level of $\mu_{\Delta} = 7.85$ for the column as observed in the as-built tests, namely $\mu_{\Delta} = 11.775$.

4.5.2 Flexural Plastic Hinge Confinement Requirements:

The analytical plastic hinge length is the length near the critical flexural section over which curvature is assumed constant to calculate plastic rotation.

4.5.3 Plastic Hinge Length, Lp

The analytical plastic hinge length is calculated using AASHTO (2011) provisions as

$$L_p=0.08L_{col} + 0.15f_yd_b \geq 0.3fyd_b \quad (4.6)$$

Where:

L_p = Plastic hinge length

L_{col} = Length of column

f_y = Tensile yield strength of steel

d_b= Diameter of longitudinal steel

Given:

L_{col} = 1828.5 mm = 72 in.

f_y= 53 ksi

d_b= 0.29 in.

Therefore,

$L_p = 0.08\ (72) + 0.15\ (53 \times 0.29) \geq 0.3\ (53 \times 0.29)$

L_p = 8.0655 in. ≥ 4.6 in.

4.5.4 Yield Curvature, Φ_y

The yield curvature can be computed according to Priestley et al. (1996):

$$\Phi_y = \lambda\varepsilon_y / D \quad (4.7)$$

Where:

λ=2.45 for spiral columns (Berry and Eberhard 2004)

ε_y=Yield strain of reinforcing steel bar

D=Diameter of column

Given:

$\varepsilon_y = f_y/E_s = 53{,}000/29000000 = 0.00183$

D= 305 mm

Therefore,

$\Phi_y = (2.45 \times 0.00183)/0.305 = 0.0147$ (1/m)

4.5.5 Required Curvature Ductility, μ_Φ

To develop the full column capacity at a demand displacement ductility, μ_Δ, the required curvature ductility, μ_Φ is computed as:

$$\mu_\Phi = 1 + (\mu\Delta - 1)/(3\ (Lp/Lcol)(1 - 0.5(Lp/Lcol)) \quad (4.8)$$

Where:

μ_Φ = Required curvature ductility

μ_Δ = Displacement ductility demand

L_p = Plastic hinge length

L_{col} = Length of column

Given:

$\mu_\Delta = 12$

L_p = 8.0655 in.= 0.205 m

L_{col} = 1.8285 m

Therefore,

$\mu_\Phi = 1 + (11.775 - 1)/(3(0.205/1.8285)(1 - 0.5(0.205/1.8285)) = 34.94$

4.5.6 Concrete Strain, ε_{cu}

The corresponding required concrete strain is computed by using Eq. (4.10)

$$\varepsilon_{cu} = \Phi_u c_u = \mu_\Phi \Phi_y c_u \tag{4.9}$$

Where:

ε_{cu} = Ultimate compression strain in concrete

Φ_u = Ultimate curvature

μ_Φ = Curvature ductility factor

Φ_y= Yield curvature

c_u = Neutral axis depth at ultimate strength of section

Given:

μ_Φ = 34.23

Φ_y = 0.0147

c_u = 6 in. = 0.1524 m

Therefore,

ε_{cu}= 34.94 x 0.0147 x 0.1524 = 0.0783

4.5.7 Compressive Strength of Confined Concrete, f_{cc}'

The compressive strength of confined concrete, f_{cc}', can be computed by Mander's (1988) stress-strain model as follows

$$f_{cc}' = f_c' \left[2.254\sqrt{1 + \frac{7.94 f_l'}{f_c'}} - \frac{2 f_l'}{f_c'} - 1.254\right] \tag{4.10}$$

Where:

fc'= Compressive strength of concrete

f_l'= Effective lateral confining stress

The effective lateral confining stress is calculated as follows

$$f_l' = k_e f_l \quad (4.11)$$

Where:

k_e = Confinement effectiveness coefficient

f_l = Lateral confining stress

The lateral confining stress is calculated as follows

$$f_l = 0.5\rho_s f_{yh} \quad (4.12)$$

Where:

p_s = Volumetric ratio of transverse reinforcement

f_{yh} = Tensile yield strength of transverse reinforcement

The volumetric ratio of transverse reinforcement, p_s, is defined as ratio of confining transverse reinforcement to the volume of confined concrete, calculated using:

$$p_s = \frac{(Asp)(\pi Dc)}{(\frac{\pi Dc.Dc}{4})S} = 4A_{sp}/D_cS \quad (4.13)$$

Where:

A_{sp} = Area of transverse reinforcement

D_c = Diameter of core, out-to-out of the transverse reinforcement

S = Center-to-center spacing of transverse reinforcement

Given:

$A_{sp} = \pi(d_{sp})^2/4 = \pi(6.6)^2/4 = 34.22$ mm^2

$D_c = 280.6$ mm

S = 50.7 mm

Therefore,

p_s = (4x34.22)/(280.6x50.7)= 0.00962

Given:

p_s = 0.00962

f_{yh} = 355 MPa

Therefore,

f_l = 0.5x0.00962x355 = 1.71 MPa

Given:

f_l = 1.71 MPa

k_e = 0.95 (for circular section according to *Priestley et al. 1996*)

Therefore,

f_l' = 0.95x1.71 = 1.62 MPa

Given:

f_l' = 1.62 MPa

f_c' = 20.68 MPa

Therefore,

$$f_{cc}' = 20.68\ [2.254\sqrt{1 + \frac{7.94(1.62)}{20.68}} - \frac{2x1.62}{20.68} - 1.254] = 30.2 \text{ MPa}$$

4.5.8 Jacket Thickness in Primary Confinement Region, t_{c1}

The jacket thickness required to provide this ultimate concrete strain determined by Eq. (4.9) is computed as:

$$t_{c1} = 0.09 \frac{D\ (\varepsilon cu - 0.004) fc'}{\Phi f\ .\ fju\ .\varepsilon ju}. 2 \qquad (4.14)$$

Where:

t_{c1} = jacket thickness in primary confinement region

D = diameter of column

ε_{cu} = ultimate compression strain in concrete

Φ_f = flexural strength reduction factor

f_{ju} = ultimate unidirectional tensile strength of jacket retrofit

ε_{ju} = ultimate tensile failure strain of jacket retrofit

$f_{cc'}$ = compressive strength of confined concrete

Given:

D = 305 mm

ε_{cu} = 0.0783

Φ_f = 0.90

f_{ju} = 4000 MPa (SikaWrap-230C)

ε_{ju} = 0.018 (SikaWrap-230C)

$f_{cc'}$ = 1.5 x 20.68 = 30 MPa

Therefore,

$$t_{c1} = 0.09 \frac{305\ (0.0783 - .004) \times 30.2}{0.9 \times 4000 \times 0.018}.2 = 1.90 \text{ mm}$$

4.5.9 Jacket Thickness in Secondary Confinement Region, t_{c2}

According to Sika Product data sheet, thickness of SikaWrap-230C laminate impregnated with Sikadur 330 is 1 mm. Hence, jacketing the damaged specimen with two layers of CFRP is sufficient to achieve defined retrofit objective.

The jacket thickness required in the secondary confinement region is given by:

$$t_{c2} = t_{c1}/2 \qquad (4.15)$$

Therefore,

t_{c2} = 1.90/2 = 0.95 mm

4.5.10 Structural Detailing

The length of primary confinement region, Lp1 and secondary confinement region, Lp2 is calculated as (Seible, et al., 1997).

Lp1 = larger of {L/8, D/2}

Lp2 = larger of {L/8, D/2}

Lp1=Lp2=larger of {72/8 in., 12/2 in.}= 9 in.

4.5.11 Design Summary

Table 4.9: Design summary

Design Summary	
Type of confinement	Spiral (Pier 2)
Displacement ductility observed in the as-built tests, μ_Δ	7.85
Ductility enhancement factor	1.5
Desired displacement ductility, μ_Δ	11.775
Jacket thickness in primary confinement region, t_{c1}	1.90 mm
Jacket thickness in secondary confinement region, t_{c2}	0.95 mm
Number of fiber wraps required in primary confinement region	2
Number of fiber wraps required in secondary confinement region	1
Length of primary confinement region for plastic hinge, L_{c1}	205 mm
Length of secondary confinement region adjacent to plastic hinge, L_{c2}	205 mm

Figure 4. 8: Retrofitted specimen with two layers of CFRP jackets at hinge location.

4.6 Experimental Testing

4.6.1 Understanding of Lab Equipment's

Shake table dynamic testing, quasi-static monotonic testing, and quasi-static cyclic testing are all possible in the laboratories of the Civil Engineering Department. It was regarded as fundamental to initially gain knowledge of the tools that will be needed in order to calibrate various devices. Various cutting-edge equipment's available in the structural laboratory of the MCE, NUST were utilized in order to test the trial bridge columns. Understanding the limitations of various testing instruments and how they influence boundary conditions was also aided by this study. A complete comprehension of the instrumentation procedure and data processing of the experimental results was a byproduct of this activity.

4.6.2 Quasi-Static Cyclic Test

With a 50-ton loading capacity, one linear hydraulic actuator was used for the quasi-static cycle testing. The structural testing frame that includes this actuator is detailed in previous chapter 3 and its features presented in Table 4.10.

Table 4.10: Specifications of actuator

Actuator 50 ton	
Capacity	500 kN
Stroke	500 mm
Type	Parkor
Maximum Speed	1 m/sec
Total length	1.53 m

4.6.3 Test Setup

Figure 4.9 shows the general setup used to test the specimens. The base of the specimens was rigidly attached/fixed to the structural floor of the lab using high-strength steel bolts. An axial load of 192.4 kN was applied on the pier header using concrete blocks fixed with bolts. This led to a normalized load ratio of 0.13, which is typical of bridge piers found in Pakistan. Quasi-static lateral cyclic load was applied in displacement control using a horizontal actuator fixed to the header block using four anchors of 20 mm diameter.

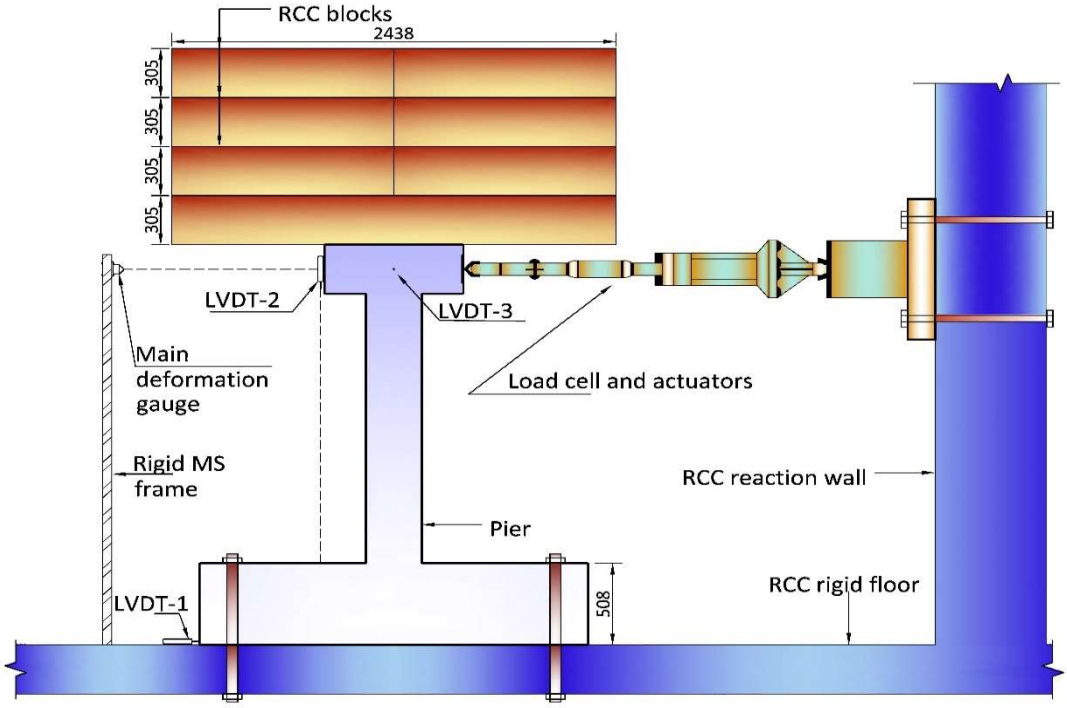

Figure 4.9: Test setup for specimen.

4.6.4 Design of Anchoring System

The anchors were required in two spots on the test specimen. The first was the column base, which was secured with a robust floor that was 12 inches thick, and the second was an 8-foot square slab that was fastened to the pedestal at the top of the column. In all situations, the estimated forces were used to determine the diameter of the anchors. The geometric criteria established the length of the anchors.

Figure 4.10 illustrates the four anchoring bolts for the column base, each of which was 44 inches long and 1.75 inches in diameter. Figure 4.10 displays the four anchor bolts for an 8 foot square slab, each measuring 27 inches in length and 1 inch in diameter. Both anchor bolts were made of mild steel and had a 40 ksi yield strength.

Figure 4.10: Test setup for specimen.

4.6.5 Displacement Transducers

With the aid of a string-potentiometer and an LVDT, the displacement at the top of the column at the moment of application of the lateral load was measured. These transducers had a resolution of roughly 0.05 mm.

Figure 4.11: Linear variable differential transformer (LVDT).

4.6.6 Data Acquisition Systems

The data was captured using the UCAM-70 data gathering system during the quasi-static cyclic testing. This system has 30 channels and is appropriate for quasi-static testing. The data for this study was sampled at a frequency of about 1.5 Hz. It is crucial to keep in mind that the cyclic testing frequency was around 0.0067 Hz, demonstrating that the sampling frequency was significantly higher than the Nyquist-Shannon sampling frequency. Although 0.067 Hz was the chosen minimum required sampling frequency and 0.0134 Hz was the theoretical minimum required sampling frequency (Dally, Riley, & McConnell, 2004), actual sampling was carried out more than 22 times the lowest required frequency. In Figure 4.12, the data acquisition system is displayed.

Using the data gathering system DR-4000, the dynamic response of the column caused by natural and forced vibration was measured. Since the response of the system being measured was less than 1.5 Hz and the data were sampled at 100 Hz for the ambient and forced vibration testing, the system also complied with the Nyquist principle.

Figure 4.12: Data Acquisition system.

4.6.7 Test Protocol

The load procedure included three push-pull cycles repeated three times at drift ratios of 0.1%, 0.3%, 0.5%, 0.6%, 0.7%, 1.0%, 2.0%, 2.5%, 3.0%, 3.5%, 3.5%, 4.0%, and 4.5%, where δ=column displacement/column length, measured from the top of the base to the point of load application. The push direction (+) was applied to each cycle before the pull direction (-). A grid of 50mm squares was drawn on the surface of the specimens to monitor the development of cracks during the test's various phases. At every cycle of the test, the growth and development of cracks were continuously observed. The tests were terminated when the load in any direction reached 80% of the test's peak load.

The lateral displacement at the header block in the testing direction was detected by an LVDT (linear variable displacement transducer) (Figure 4.9). Potential base horizontal movement, vertical displacements, and potential header out-of-plane movement were all measured by three more LVDTs. Before applying the load cycles, a digital accelerometer was positioned in the middle of the concrete blocks to perform free vibration experiments. A computerized data acquisition system was used to record the test results.

Chapter 5

Experimental Results and Conclusions

5.1 Introduction

In this chapter, results are presented of quasi static cycling test accomplished on the solid circular reinforced concrete bridge column specimen of scale factor 4. The dynamic properties of specimen performing under internal and external confinement and damages are observed throughout the test. The test results i.e. hysteresis loop, backbone curve, energy dissipation, and stiffness degradation are presented in details.

5.2 Quasi-Static Cyclic Test

The quasi-static testing of pier specimen was completed following the protocol defined in previous chapter. Three cycles per drift and total of 37 cycles till failure at 4.5% drift were the key characteristics of testing. A push force of actuator acting in the north direction is referred to as a positive force, whilst a pull force operating in the south direction of the test specimen is described as a negative force. Similarly, positive displacement is employed to depict column movement in the north and negative displacement serves to represent movement in the south direction. The values of peak lateral load and peak displacement are recorded which are displayed below in Table 5.1.

Table 5.1: Data Takeoff Sheet for the Cyclic Test

Data Takeoff Sheet For The Cyclic Test								
Sr	**Drift (%)**	**Displacement (mm)**	**Cycle**	**Lateral Load**				
1	0.1	1.8285			Push(+)	Pull(-)	Pull(-)	Push(+)
			Cycle 1	P (kN)	4.75	0	-5.28	0
			Cycle 2	P (kN)	4.72	0	-5.31	0
			Cycle 3	P (kN)	4.69	0	-5.32	0
2	0.3	5.4855			Push(+)	Pull(-)	Pull(-)	Push(+)
			Cycle 1	P (kN)	11.62	0	-13.50	0

			Cycle 2	P (kN)	11.49	0	-13.49	0
			Cycle 3	P (kN)	11.47	0	-13.47	0
3	0.5	9.1425			Push(+)	Pull(-)	Pull(-)	Push(+)
			Cycle 1	P (kN)	19	0	-20	0
			Cycle 2	P (kN)	18.81	0	-19.77	0
			Cycle 3	P (kN)	18.93	0	-19.79	0
4	0.6	10.971			Push(+)	Pull(-)	Pull(-)	Push(+)
			Cycle 1	P (kN)	10.44	0	-11.62	0
			Cycle 2	P (kN)	10.69	0	-11.56	0
			Cycle 3	P (kN)	10.65	0	-11.55	0
5	0.75	13.71375			Push(+)	Pull(-)	Pull(-)	Push(+)
			Cycle 1	P (kN)	16.72	0	-15.88	0
			Cycle 2	P (kN)	16.03	0	-15.19	0
			Cycle 3	P (kN)	16.09	0	-14.92	0
6	1	18			Push(+)	Pull(-)	Pull(-)	Push(+)
			Cycle 1	P (kN)	21.25	0	-19.37	0
			Cycle 2	P (kN)	21.44	0	-19.56	0
			Cycle 3	P (kN)	21.39	0	-19.37	0
7	1.5	27.4275			Push(+)	Pull(-)	Pull(-)	Push(+)
			Cycle 1	P (kN)	31.12	0	-24.19	0
			Cycle 2	P (kN)	30.69	0	-23.67	0
			Cycle 3	P (kN)	30.50	0	-23-36	0
8	2	36.57			Push(+)	Pull(-)	Pull(-)	Push(+)
			Cycle 1	P (kN)	38.68	0	-25.12	0
			Cycle 2	P (kN)	37.79	0	-24.44	0
			Cycle 3	P (kN)	37.50	0	-24	0
9	2.5	45.7125			Push(+)	Pull(-)	Pull(-)	Push(+)
			Cycle 1	P (kN)	41.87	0	-21.57	0
			Cycle 2	P (kN)	41.69	0	-21.44	0
			Cycle 3	P (kN)	40.94	0	-20.94	0
10	3	54.855			Push(+)	Pull(-)	Pull(-)	Push(+)
			Cycle 1	P (kN)	44.56	0	-21.12	0
			Cycle 2	P (kN)	42.90	0	-20.44	0

			Cycle 3	P (kN)	41.72	0	-20	0
11	3.5	63.9975			Push(+)	Pull(-)	Pull(-)	Push(+)
			Cycle 1	P (kN)	44.37	0	-18	0
			Cycle 2	P (kN)	42.48	0	-16.94	0
			Cycle 3	P (kN)	40.77	0	-16.05	0
12	4	73.14			Push(+)	Pull(-)	Pull(-)	Push(+)
			Cycle 1	P (kN)	44.07	0	-17.81	0
			Cycle 2	P (kN)	43.33	0	-15.23	0
			Cycle 3	P (kN)	41.43	0	-14.09	0
13	4.5	82.2825			Push(+)	Pull(-)	Pull(-)	Push(+)
			Cycle 1	P (kN)	41.20	0	-13.65	0
			Cycle 2	P (kN)	37.27	0	-10.92	0
Test stopped due to strength degradation								

5.3 Observed Damage

The testing initiated with one cycle of 0.1% drift followed by the remaining two cycles of first drift. After completing the first drift, three cycles of each 0.3%, 0.5%, 0.6% and 0.75% drifts was applied and pier damage behavior was monitored through each cycle. Square boxes of 50 mm x 50 mm was drawn on the entire length of column to easily monitor the cracks and damages. Around 0.6% drift level, minor and hardly visible hair line cracks were observed. At 1.5% drift, the north and south faces of the column started to display visible cracks, which are seen in Figure 5.1. At this point, the maximum restoring force was (+) 33.69 kN in the north and (-) 6.76 kN in the south. This point is the initial yield point, which implies that at 1.5% drift (27.48 mm), the steel began to yield, which is also clear from the analysis of hysteresis curve.

Further analysis of the data plotted for the displacement hysteresis curves reveals that the initial concrete cracking occurred at approximately 0.46% drift, the initial yield at 1.5%, and the yield at 2.02% for the force applied in the north direction. The cracking occurred at 0.47% drift, the initial yield at 1.44%, and the yield at 1.58% for the force applied in the south direction, as shown by the plot of the backbone curve in Figure 5.2. Table 5.2 lists the values for yield, initial yield, and cracking.

The un-cracked stiffness, cracked stiffness, and equivalent stiffness are determined using the observations and data mentioned above. As defined, the un-cracked stiffness is given by:

$$Kuc = \frac{Pc}{Uc}$$

Where:

k_{uc} is referred to un-cracked stiffness.

P_c is referred to load at cracking.

u_c is the corresponding cracking displacement.

From the above equation two values of uncracked stiffness are determined one for the pushing force when applied in north direction and other for pulling force in south direction, the uncracked stiffness for north direction was 10.28 k/in and for south direction it was 11.87 k/in. These values are presented in Table 5.2. Also the cracked stiffness is defined as:

$$Kcr = \frac{Pyo}{Uyo}$$

Where:

k_{cr} is defined as cracked stiffness.

P_{y0} is defined as load at initial yield.

u_{y0} is the initial yield corresponding displacement.

The cracked stiffness values for the north and south directions are11.48 kips/in and 12.50 kips/in, respectively. These values are given in Table 5.2.

The cracks on the north and south faces of the column continued to grow at 2% drift after adding three additional cycles per drift.

After applying three more cycle at 2.5% drift, significant cracks was seen in the CFRP jackets at the north and south face of column. Reinforcement bars are believed to have buckled at this drift level, especially along the south face.

The both north and south faces of column at 3% drift shows the significant breaking of CFRP jackets fibers and buckling/twisting of steel bars is also believed to be occur and in yielding process at this stage. The breaking of jackets fiber were shown at both primary and secondary layers in the plastic hinge zone.

At final drift level of 4.5% the fiber of primary and secondary jackets further broke. It is essential to remember that at 4.5% drift, only two cycles could be performed because the column's strength was severely degraded. As a result, further testing was stopped.

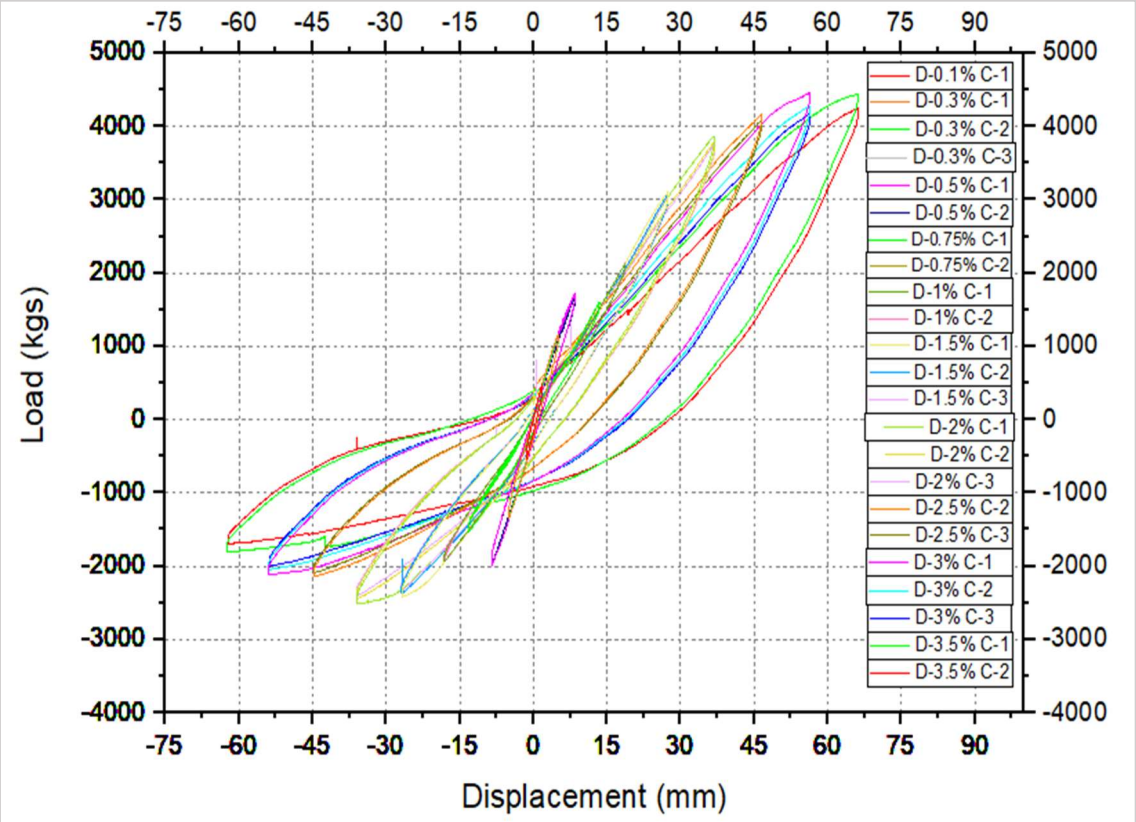

Figure 5.1: Hysteresis loop of column specimen

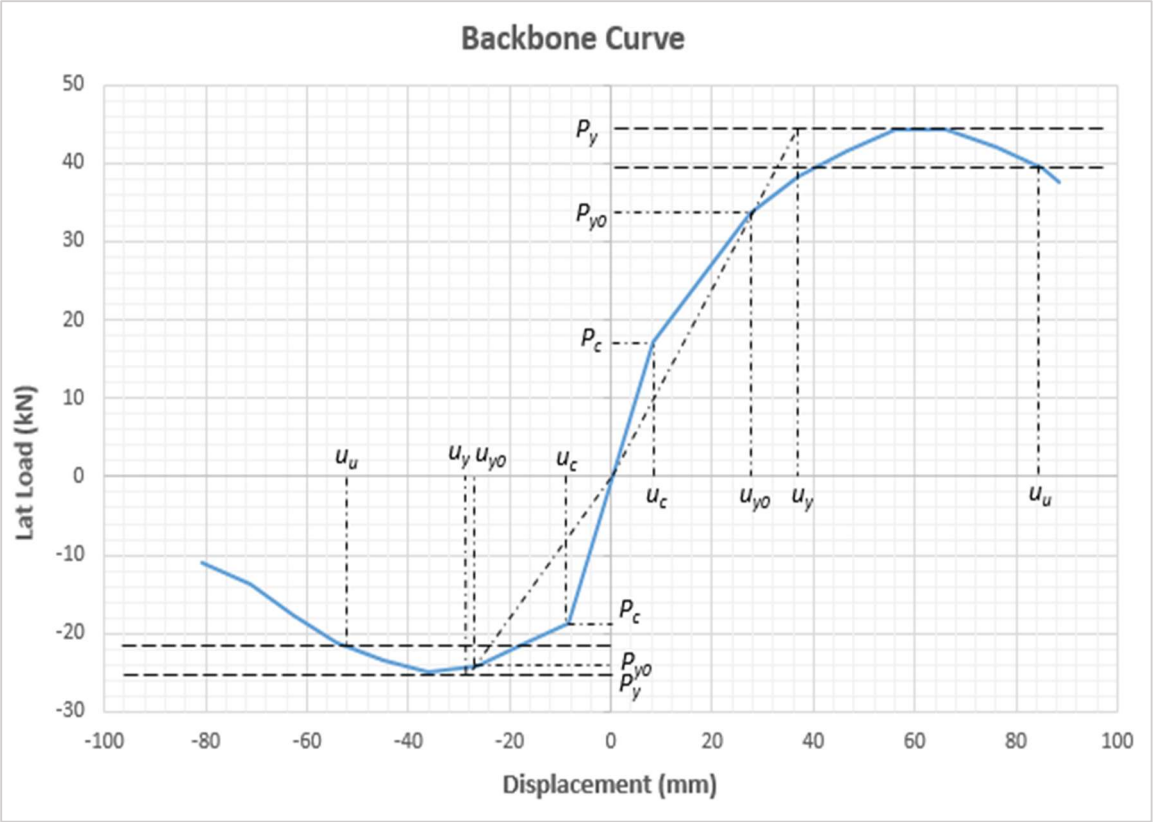

Figure 5.2: Backbone curve of column specimen

Table 5.2: Cracking, initial yield and yield values for column

Item	**North Direction Values**	**South Direction Values**
P_c	17.06 kN	-18.64 kN
u_c	0.46% (8.48 mm)	-0.47% (-8.50 mm)
k_{uc}	2.01 kN/mm (11.48 kips/in)	2.19 kN/mm (12.50 kips/in)
Equivalent k_{uc}	2.10 kN/mm (11.99 kips/in)	
P_{y0}	33.69 kN	-24.12 kN
u_{y0}	1.5% (27.48 mm)	-1.44% (-26.47 mm)
K_{cr}	1.22 kN/mm (6.97 kips/in)	0.91 kN/mm (5.17 kips/in)
Equivalent k_{cr}	1.06 kN/mm (6.05 kips/in)	
P_y	44.37 kN	-25 kN
u_y	2.02% (36.87 mm)	-1.58% (-28.93 mm)
u_{max}	4.41%	
μ_d	3.20	

5.4 Energy Dissipation

The hysteresis curves were plotted using the load-deformation data, and the amount of energy dissipated during each cycle was computed. Hysteresis curves corresponding to 0.50%, 1.0%, 2.0%, 3.0%, 3.50%, 4.0%, and 4.50% for various stages of cyclic testing.

It was observed that as drift level increased, the amount of energy dissipated every cycle increased as well. The first cycle of 4.50% drift indicate the maximum energy dissipation. Further observation reveals that the first cycle dissipates more energy than the second or third cycle, with the difference between the second and third cycles being less.

Table 5.3 lists the energy dissipated per cycle and total energy dissipated data. Figure 5.3 shows the energy dissipated per cycle. It is clear from this figure that energy dissipation begins at roughly 1.50% drift, which is in line with previous talks of section 5.3 in which the yield point was established. It is important to note that energy dissipation only occurs when the system yields and in elastic state there is no or very less hysteretic energy dissipation before that.

Figure 5.4 depicts the cumulative energy graph, with a polynomial function defining the curve. It is significant to observe that in this column, 36 cycles were completed before failure, which occurs at 4.40%.

Table 5.3: Energy dissipation for column specimen

Drift (%)	Cycle	Energy Dissipation per Cycle (k-in)	Cumulative Energy Dissipation (k-in)
0.1%	1	0.048	0.048
	2	0.039	0.087
	3	0.034	0.122
0.3%	1	0.227	0.349
	2	0.204	0.552
	3	0.197	0.749
0.5%	1	0.446	1.195
	2	0.393	1.589
	3	0.370	1.959

0.6%	1	0.401	2.360
	2	0.375	2.735
	3	0.368	3.102
0.75%	1	0.463	3.565
	2	0.449	4.014
	3	0.509	4.522
1%	1	0.747	5.269
	2	0.742	6.011
	3	0.727	6.738
1.5%	1	2.158	8.896
	2	2.017	10.913
	3	1.995	12.908
2%	1	4.857	17.765
	2	4.566	22.331
	3	4.456	26.787
2.5%	1	8.179	34.966
	2	7.589	42.555
	3	7.139	49.694
3%	1	11.630	61.324
	2	11.061	72.385
	3	10.716	83.101
3.5%	1	15.421	98.522
	2	14.178	112.700
	3	13.561	126.261
4%	1	18.103	144.364
	2	16.703	161.068
	3	16.010	177.078
4.5%	1	13.848	190.926
	2	5.359	196.285
Test stopped due to strength degradation.			

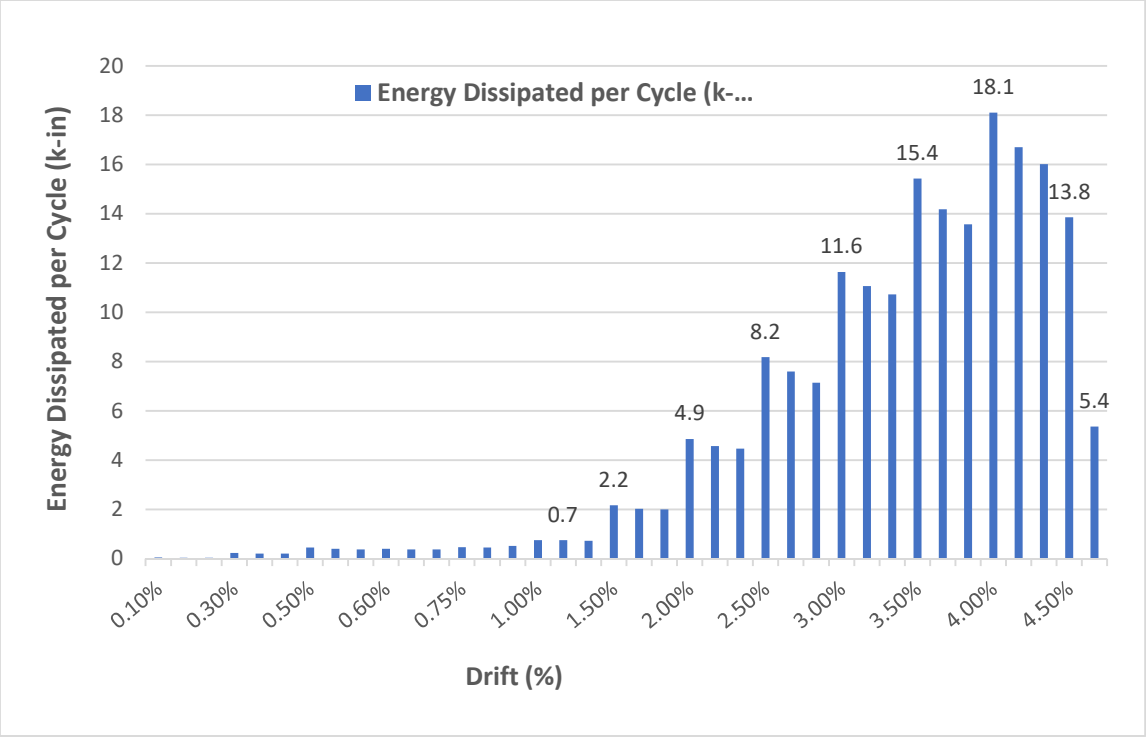

Figure 5.3: Energy Dissipated per Cycle (k-in) of column

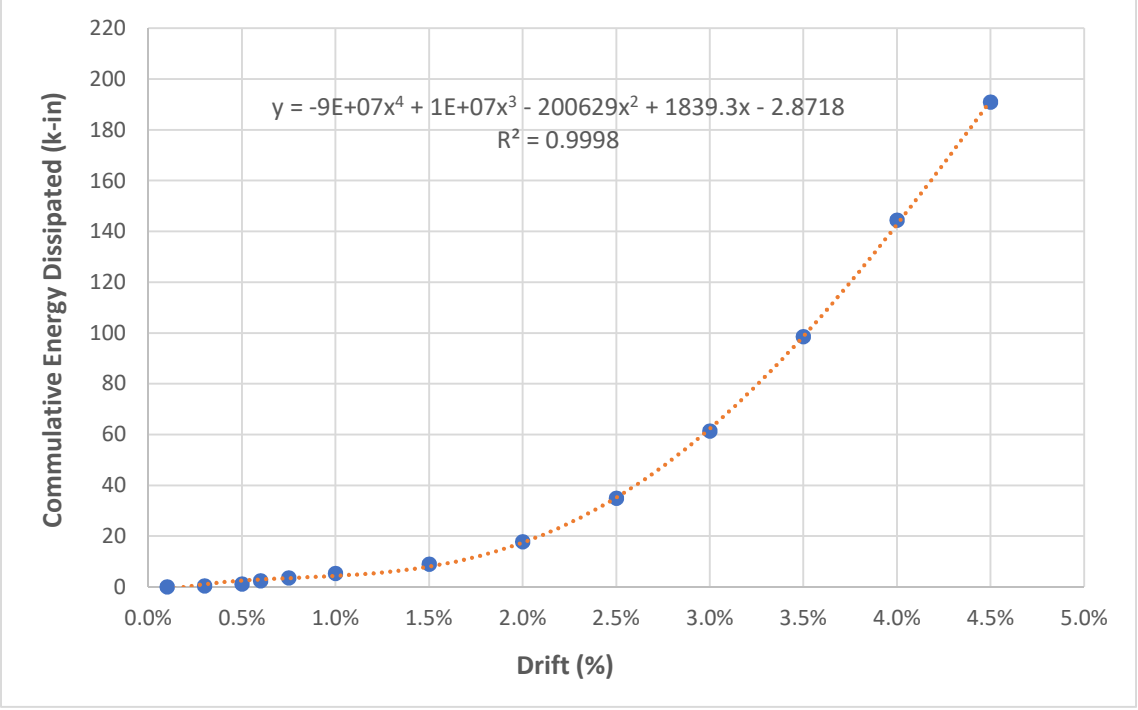

Figure 5.4: Cumulative Energy Dissipation (k-in)

5.5 Stiffness Degradation

For each loop of hysteresis, the equivalent stiffness can be calculated using the hysteresis data received from the cycling testing using below equation (Kawashima K., 2006).

$$Ke = \frac{Pmax - Pmin}{Umax - Umin}$$

Figure 5.19 illustrates the stiffness deterioration graph for this column and includes a polynomial equation for the curve. In this instance, it's crucial to note that the initial-to-final stiffness ratio in this case is 8.24, indicating a major stiffness degradation of the section at 4.50% drift.

Table 5.4: Stiffness degradation values for column

Drift	Stiffness (kips/in)
0.10 %	15.66
0.30 %	12.55
0.50 %	9.68
0.60 %	8.08
0.75 %	7.41
1.00 %	6.44
1.50 %	5.76
2.00 %	4.98
2.50 %	3.96
3.00 %	3.42
3.50 %	2.78
4.00 %	2.42
4.50 %	1.90

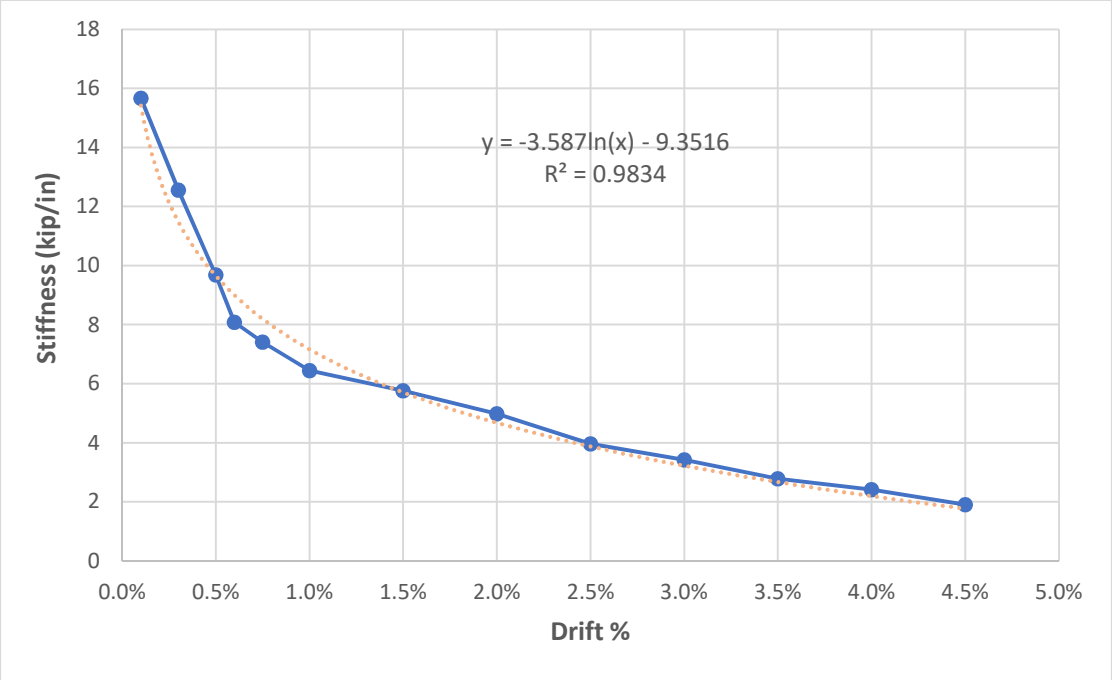

Figure 5.5: Stiffness degradation curve

Chapter 6

Summary and Conclusions

5.1 Summary

Bridges are unique structures because they support a significant amount of mass at the top of a column. Large inertial forces are created during an earthquake motions and their energy must be released. The energy contributed by smaller earthquakes is dispersed elastically by damping, while the energy delivered by major seismic activity is dispersed by inelastic action created in the bridge piers. Hysteretic energy dissipation in concrete is a complicated phenomenon that is affected by a wide range of variables. While many experts have attempted to explain this phenomenon, there are still questions that need to be answered.

This research was conducted to explore and comprehend the energy dissipation via hysteresis in low or average strength reinforced concrete bridge columns which is currently unexplored. The study's main contributions are the estimation of a response modification factor utilized in the design of bridge columns, as well as the calculation of associated parameters such as ductility, energy dissipation, stiffness degradation, and graphing load-drift response. In addition, the column resilience of a bridge is quantified by using CFRP jackets as external confinement in the maximum bending movement area which is plastic hinge region near the base of the column.

This article investigates experimentally the cyclic behavior of one circular RC pier internally confined with pre-bent metal strips. The geometry and detailing of the tested specimens replicate RC piers of typical bridges currently built in Pakistan. The results are discussed in terms of observed damage, lateral capacity, ductility, stiffness degradation and equivalent viscous damping. This article contributes towards developing new and more effective confinement solutions for RC piers of bridges built in seismic-prone developing countries.

5.2 Conclusions

Some of previous test results of model column were not available due to some reasons and column specimen was found in failure state in MCE, NUST structural lab. Therefore it was difficult to compare the complete test results with the previous one and few results are compared. In light of the test model's low strength concrete and its degraded state before the specimen was repaired and retrofitted with CFRP, the following conclusions were obtained:

1) It was determined that the ductility of the retrofitted low-concrete-strength circular RC bridge piers strengthened by CFRP was greater than that of the original RC bridge piers, which also failed at a drift of 4.5%. LSC RC bridge piers retrofitted with external confinement behave similar to that of regular and high-strength concrete in terms of both strength and ductility. Low strength RC bridge piers have a better seismic response after being retrofitted.
2) Tests were conducted on severely damaged bridge model. After proper repairs and retrofitting, even a severely damaged RC bridge pier can not only regain its previous strength but also resist a significantly larger seismic event, as demonstrated experimentally.
3) Around 0.6% drift level, minor and hardly visible hair line cracks were observed. Visible cracks started to appear at the north and south face of the column at 1.5% drift level.
4) At a drift rate of 1.5%, the maximum restoring force was +33.69 kN in the north direction and -6.76 kN in the south direction. The assessment of hysteresis curves reveals that this is the initial yield point, indicating that steel began to yield at a drift of 1.5% (or 27.48 mm).
5) The plot of the backbone curve shows that for the force applied in the north direction, cracking occurred at about 0.46 % drift, initial yield was at 1.5 %, and yield was at 2.02 %, while for the force applied in the south direction, cracking occurred at 0.47 % drift, initial yield was at 1.4 %, and yield was at 1.5 %.

6) At a 2% drift level, it was discovered that the retrofitted column's ductility was up to 24% more than that of the original column.
7) It was observed that as drift level increased, the amount of energy dissipated every cycle increased as well. The first cycle of 4.50% drift indicate the maximum energy dissipation. Further observation reveals that the first cycle dissipates more energy than the second or third cycle, with the difference between the second and third cycles being less of same drift level.
8) After successive cycles, enhancement in energy dissipation capability increased in retrofitted column. The cumulative energy the retrofitted column specimen dissipated is improved by up to 39.38 percent.
9) For the north direction, the cracked stiffness value was determined to be 11.48 kips/in, whereas the value for the south direction was 12.50 kips/in. A significant degradation of stiffness in the column can be seen at 4.50% drift, as indicated by the ratio of initial to final stiffness which is 8.24.

5.3 Recommendations

The following studies are suggested for further investigation.

1. To investigate the effect of seismic response of square bridge piers having comparatively low and average concrete strength.
2. It is recommended that various retrofitting techniques be researched for the current stock of bridge piers available in MCE, NUST structural lab which do not adhere to seismic regulations.
3. To develop most economical retrofitting technique by drawing comparison between other methods of strengthening of bridge pers.
4. This study was focused on strengthening the plastic hinge region of piers. It is suggested to study the effect of CFRP jackets upon the whole length of column.

REFERENCES

AASHO. (1961). *AASHO Standard Specifications for Highway Bridges, 8th Edition.* Washington, D.C.: Association General Offices, 917 National Press Building, Washington 4, D.C.

AASHTO. (2009). *AASHTO Guide Specifications for LRFD Seismic Bridge Design-1st Edition.* American Association of State Highway and Transportation Officials.

AASHTO. (2007). AASHTO LRFD Design Specifications 4th Edition. American Association of State Highway and Transportation Officials.

AASHTO. (2002). *Standard Specifications for Highway Bridges 17th Edition.* Washington D.C.: American Association of State Highway and Transportation Officials.

ACI 318-02. (2001, November 1). *Building Code Requirements for Structural Concrete*. USA: American Concrete Institute.

ASTM A615/A615M-03a. (2004, January). *Standard Specification for Deformed and Plain BilletSteel Bars for Concrete Reinforcement.* West Conshohocken, Pennsylvania, USA: American Society for Testing and Materials.

ASTM C109/C109M-02. (2004, October). *Standard Test Method for Compressive Strength of Hydraulic Cement Mortars.* West Conshohocken, Pennsylvania, USA: American Society for Testing and Materials.

ASTM C117-04. (2004, October). *Standard Test Method for Materials Finer than 75-µm (No. 200) Sieve in Mineral Aggregates by Washing.* West Conshohocken, Pennsylvania, USA: American Society for Testing and Materials.

ASTM C128-04. (2004, October). *Standard Test Method for Density, Relative Density (Specific Gravity), and Absorption of Fine Aggregate.* West Conshohocken, Pennsylvania, USA: American Society for Testing and Materials.

ASTM C136-04. (2004, October). *Standard Test Method for Sieve Analysis of Fine and Coarse Aggregates.* West Conshohocken, Pennsylvania, USA: American Society for Testing and Materials.

ASTM C150-04. (2004, October). *Standard Specification for Portland Cement.* West Conshohocken, Pennsylvania, USA: American Society for Testing and Materials.

ASTM C188-95(2003). (2004, October). *Standard Test Method for Density of Hydraulic Cement.* West Conshohocken, Pennsylvania, USA: American Society for Testing and Materials.

ASTM C191-04a. (2004, October). *Standard Test Method for Time of Setting of Hydraulic Cement by Vicat Needle.* West Conshohocken, Pennsylvania, USA: American Society for Testing and Materials.

ASTM C78-02. (2004, October). *Standard Test Method for Flexural Strength of Concrete (Using Simple Beam with Third-Point Loading).* West Conshohocken, Pennsylvania, USA: American Society for Testing and Materials.

ASTM C873-04. (2004, October). *Standard Test Method for Compressive Strength of Concrete Cylinders Cast in Place in Cylindrical Molds.* West Conshohocken, Pennsylvania, USA: American Society for Testing and Materials.

ATC and MCEER. (2003). *Recommended LRFD Guidelines for the Seismic Design of Highway Bridges (MCEER/ATC-49).* Buffalo NY: Multidisciplinary Center for Earthquake Engineering Research (MCEER-03-SP03).

Bae, S., & Bayrak, O. (2008). Seismic Performance of Full-Scale Reinforced Concrete Columns. *ACI Structural Journal, 105* (2), 123-133.

Bayrak, O., & Sheikh, S. A. (2001). Plastic Hinge Analysis. *Journal of Structural Engineering, 127* (9), 1092-1100.

BCP. (1986). *Building Code of Pakistan.* Islamabad: Ministry of Housing, Govt. of Pakistan.

BCP. (2007). *Building Code of Pakistan: Seismic Provisions.* Islamabad: Ministry of Housing, Govt. of Pakistan.

Bouc, R. (1967). Forced Vibration of Mechanical Systems with Hystersis. *4th Conference on Nonlinear Oscillations.* Prague.

Bracci, J. M. (1992). *Experimental and Analytical Study of Seismic Damage and Retrofit of Lightly Reinforced Concrete Structures in Low Seismicity Zones.* Buffalo: State University of New York.

Chen, Y., Feng, M. Q., & Soyoz, S. (2008). Large-Scale Shake Table Test Verification of Bridge Condition Assessment Methods. *Journal of Structural Engineering, 7*, 1235-1245.

Cheok, G. S., & Stone, W. C. (1990). Behavior of 1/6-Scale Model Bridge Columns Subjected to Inelastic Cyclic Loading. *ACI Structural Journal, 87* (6), 630-638.

Chopra, A. K. (2001). Fast Fourier Transform. In A. K. Chopra, *Dynamics of Structures Theory and Applications to Earthquake Engineering* (2nd ed., pp. 796-800). New Jersy, USA: Prentice-Hall Inc.

Chopra, A. K. (2001). Free Vibration Tests. In A. K. Chopra, *Dynamics of Structures Theory and Applications to Earthquake Engineering* (2nd ed., pp. 54-55). New Jersy, USA: Prentice-Hall Inc.

Durrani, A. J., Elnashai, A. S., Hashash, Y. M., Kim, S. J., & Masud, A. (2005). *The Kashmir Earthquake of October 8, 2005-A Quick Look Report.* Urbana-Champaign: MAE Center.

Eberhard, M. O., Stanton, J. F., & Trochalakis, P. (1996). Design of Seismic Restrainers. *Fourth National Workshop on Bridges Research in Progress*, (pp. 283-286). Buffalo, New York.

EERI. (2006, February). *Learning from Earthquakes - Special Report - The Kashmir Earthquake of October 8, 2005: Impacts in Pakistan*. Retrieved January 17, 2009, from Earthquake Engineering Research Institute: http://www.eeri.org/lfe/pdf/kashmir_eeri_2nd_report.pdf

Fujikura, S., Kawashima, K., Shoji, G., Zhang, J., & Takemura, H. (2000). Effect of the Interlocking Ties and Cross Ties on the Dynamic Strength and Ductility of Rectangular Reinforced Concrete Bridge Columns. *Journal of Structural Mechanics and Earthquake Engineering, 640* (I-50), 71-88.

Ghobarah, A., & Tso, W. K. (1973). Seismic Analysis of Skewed Highway Bridges with Intermediate Support. *Earthquake Engineering and Structural Dynamics, 2* (3), 235-248.

Gobarah, A., & Ali, H. M. (1988). Seismic Performance of Highway Bridges. *Engineering Structures, 10* (3), 157-166.

Kawashima, K. (2006). *Seismic Design, Isolation and Retrofit of Bridge.* Tokyo: Department of Civil Engineering Tokyo Institute of Technology, Japan.

Kawashima, K. (2000). Seismic Performance of RC Bridge Piers in Japan: An Evaluation after the 1995 Hyogo-Ken Nanbu Earthquake. *Prog. Struct. Engng. Mater.* (2), 82-91.

Mander, J. B., Waheed, S. M., Chaudhary, M. T., & Chen, S. S. (1993). *Seismic Performance of Shear-Critical Reinforced Concrete Bridge Piers.* Buffalo, NY: National Center for Earthquake Engineering Research (NCEER), SUNY.

Meyer, C. (1989). Inelastic Seismic Analysis of Concrete Buildings. *Seismic Engineering Research Practice,* 837-846.

Meyer, C., Roufaiel, M. S., & Arzoumanidis, S. G. (1983). Analysis of Damaged Concrete Frames for Cyclic Loads. *Earthquake Engineering & Structural Dynamics, 11* (2), 207-228.

Pakistan Metrological Department & NORSAR Norway. (2006). *Seismic Hazard Analysis and Zonation of Azad Kashmir and Northern Areas of Pakistan.* Islamabad: PMD.

Priestley, M. J., & Benzoni, G. (1996). Seismic Performance of Circular Columns with Low Longitudinal Reinforcement Ratios. *ACI Structural Journal, 93* (4), 1-12.

Priestley, M. J., Seible, F., & Calvi, G. M. (1996). Fundamentals of Seismic Bridge Behavior: Structural Dynamics. In *Seismic Design and Retrofit of Bridges* (pp. 173-177). New York: John Wiley & Sons Inc.

Sheikh, S. A. (1978). *Effectiveness of rectangular ties as confinement (PhD Dissertation).* Toronto: University of Toronto.

Syed, A. M. (2008, November 14). *(~GEEC06.kmz) Bridges & Kashmir Earthquake of Oct. 2005*. Retrieved January 22, 2009, from Google Maps: http://maps.google.com/maps?q=http://bbs.keyhole.com/ubb/download.php?Number=1258144&t=k&om=1

Syed, A. M. (2008, November 14). *Bridges & Earthquake of Oct. 8, 2005 Pakistan*. Retrieved January 22, 2009, from Google Earth Community: http://bbs.keyhole.com/ubb/ubbthreads.php?ubb=showflat&Number=1174014#Post1174014

Syed, A. M. (2008, December). Specialized Training on Structural Dynamic Testing Facility at SEESL Buffalo. Buffalo, New York, USA.

Syed, A. M., & Shakal, A. (2007). *Response to the Pakistan Earthquake of October 8, 2005*. Retrieved December 19, 2008, from The National Acadmies: www7.nationalacademies.org/dsc/Quake_Report_2007.pdf

Syed, A. M., Khan, A. N., Ali, Q., Javed, M., Mohammad, A., Ahmad, I., et al. (2006). Performance of Engineered & Non-engineered Structures in Northern Pakistan & AzadKashmir during Oct 8 EarthquakeEarthquake. *100th Anniversary Earthquake Conference: 8NCEE. SSA-866.* San Francisco: EERI, SSA, OES and DRC.

Zelinski, R. J., & Dubovik, A. T. (1991). Seismic Retrofit of Highway Bridge Structures. *Lifeline Earthquake Engineering: 3rd US Conference* (pp. 11-120). New York, NY: ASCE New York.